Diffusion-controlled annihilation $A + B \rightarrow 0$: Coalescence, fragmentation, and collapse of nonidentical A-particle islands submerged in the B-particle sea

Boris M. Shipilevsky ⬤

Institute of Solid State Physics, Chernogolovka, Moscow District 142432, Russia

We present a systematic analysis of diffusion-controlled interaction and collapse of two nonidentical spatially separated d-dimensional A-particle islands in the B-particle sea at propagation of the sharp reaction front $A + B \rightarrow 0$ at equal species diffusivities. We show that at a sufficiently large initial distance between the centers of islands 2ℓ and a relatively large initial ratio of island-to-sea concentrations, the evolution dynamics of the island-sea-island system demonstrates remarkable universality and, depending on the system dimension, is determined unambiguously by two dimensionless parameters $\Lambda = \mathcal{N}_0^+/\mathcal{N}_\Omega$ and $q = \mathcal{N}_0^-/\mathcal{N}_0^+$, where $\mathcal{N}_0^+$ and $\mathcal{N}_0^-$ are the initial particle numbers in the larger and smaller of the islands, respectively, and $\mathcal{N}_\Omega$ is the initial number of sea particles in the volume $\Omega = (2\ell)^d$. We find that at each fixed $0 < q \leqslant 1$, there are threshold values $\Lambda_\star(q)$ and $\Lambda_s(q) \geqslant \Lambda_\star(q)$ that depend on the dimension and separate the domains of individual death of each of the islands $\Lambda < \Lambda_\star(q)$, coalescence and subsequent fragmentation (division) of a two-centered island $\Lambda_\star(q) < \Lambda < \Lambda_s(q)$, and collapse of a single-centered island formed by coalescence $\Lambda > \Lambda_s(q)$. We demonstrate that regardless of d, the trajectories of the island centers are determined unambiguously by the parameter q, and we reveal a detailed picture of the evolution of islands and front trajectories with an increase in Λ, focusing on the scaling laws of evolution at the final collapse stage and in the vicinity of starting coalescence and fragmentation points.

I. INTRODUCTION

For the last decades the reaction-diffusion system $A + B \rightarrow 0$, where unlike species A and B diffuse and irreversibly react in a d-dimensional medium, has acquired the status of one of the most popular objects of research [1–6]. This attractively simple system, depending on the initial conditions, displays a rich variety of phenomena, and, depending on the interpretation of A and B, it provides a model for a broad spectrum of problems [7–16]. A crucial feature of many such problems is formation of the localized *reaction front* $A + B \rightarrow 0$, which propagates between domains of unlike diffusing species A and B and occurs as a consequence of their effective *dynamical repulsion*.

The simplest model of a planar reaction front, introduced by Galfi and Racz [17], is the quasi-one-dimensional model for two initially separated reactants which are uniformly distributed on the left side ($x < 0$) and on the right side ($x > 0$) of the initial boundary. Taking the reaction rate in the mean-field form $R(x, t) = ka(x, t)b(x, t)$ (k being the reaction constant), GR discovered that in the long time limit $kt \gg 1$ the reaction profile $R(x, t)$ acquires a universal scaling form with the width $w \propto (t/k^2)^{1/6}$, so that on the diffusion length scale $L_D \propto t^{1/2}$ the relative width of the front asymptotically contracts unlimitedly

$$w/L_D \propto (kt)^{-1/3} \rightarrow 0$$

as $kt \rightarrow \infty$. Based on this fact, a general concept of the front dynamics for nonzero diffusivities, the quasistatic approximation (QSA), was developed [18–22]. The key property of the QSA is that the front width $w(J)$ depends on t only through the time-dependent boundary current $J_A = |J_B| = J$, the calculation of which is reduced to solving the external diffusion problem with the moving *absorbing boundary* (Stefan problem). Following this approach, in most subsequent works the use of the QSA was traditionally restricted by the quasi-one-dimensional *sea-sea* problem with A and B domains having an unlimited extension, i.e., with unlimited number of A and B particles, where asymptotically the stage of monotonous quasistatic front propagation is always reached.

In the recent Refs. [23–31] it has been shown that based on the QSA the scope of the $A + B \rightarrow 0$ problems which allow for analytic description can be appreciably broadened including the systems where the particle number of one or both species is *finite* (island-sea and island-island systems) and, therefore, in the final state one or both islands *disappear* completely. It has been demonstrated that in the sharp-front regime these systems exhibit rich scaling behavior, and though in these systems the QSA is always asymptotically violated, at large initial particle numbers and a high reaction constant the vast majority of particles die in the *sharp-front* regime over a wide parameter range. One of the most important problems here is the evolution of the *island-sea* system, introduced originally in Ref. [23] for quasi-one-dimensional geometry (flat front) and generalized for d dimensions (ring-shaped or spherical fronts) in the recent Ref. [31]. This system is the basic model for a wide range of phenomena and is realized in numerous applications from Liesegang pattern formation [32–35] to electron-hole luminescence in quantum wells [7–9]. It has been established that at sufficiently large

reaction constant k the death of a majority of island particles $\mathcal{N}(t)$, regardless of the initial particle distribution, proceeds in the universal scaling regime

$$\mathcal{N} = \mathcal{N}_0 \mathcal{G}(t/t_c),$$

where $t_c \propto \mathcal{N}_0^{2/d}$ is the lifetime of the island in the sharp-front limit and on the final stage of collapse

$$\mathcal{N}/\mathcal{N}_0 \propto \mathcal{T}^{(d+2)/2} \to 0$$

as $\mathcal{T} = (t_c - t)/t_c \to 0$. It has been shown that at a relatively large starting ratio of island to sea concentrations, regardless of the starting particle number and the system dimension, while dying, the island first expands to certain maximal amplitude and then begins to contract by the universal law

$$\zeta_f = r_f/r_f^M = \sqrt{e\tau |\ln \tau|}, \tag{1}$$

where $\tau = t/t_c$ and $r_f^M \propto \mathcal{N}_0^{1/d}$ is the island maximal expansion radius at the front turning point $t_M = t_c/e$.

It has been established that regardless of the system dimension in the mean-field regime the relative front width $\eta = w/r_f$ changes by the law

$$\eta = \eta_M/(e\tau \ln^2 \tau)^{1/3},$$

where at the front turning point $\eta_M \propto 1/\mathcal{N}_0^{2/3d} k^{1/3}$ and, therefore, on the final stage of collapse

$$\eta \propto (\mathcal{T}_Q/\mathcal{T})^{2/3},$$

where $\mathcal{T}_Q \propto 1/\mathcal{N}_0^{1/d}\sqrt{k} \to 0$ as $\mathcal{N}_0, k \to \infty$.

According to Eq. (1), with an increase of the initial particle number in the island, the amplitude of island expansion at the front turning point increases unlimitedly and, therefore, in the presence of neighboring islands in the sea the scenario described above for the autonomous evolution of the island is realized only as long as the amplitude of the island expansion remains much less than the distance between the centers of neighboring islands. If in the sea there are one or several neighboring islands and this condition is violated, it is obvious that the dynamics of island evolution must radically change.

Recently, the problem of diffusion-controlled *interaction* of two spatially separated *identical* d-dimensional A-particle islands in the B-particle sea has been systematically investigated at equal species diffusivities in Ref. [36]. This model is the simplest basic model of the island-sea-island system which allowed revealing the key features of the evolution dynamics under the assumption of sharp-front formation. Moreover, because of mirror symmetry, this model simultaneously describes the evolution of the d-dimensional A-particle island in a semi-infinite B-particle sea with a reflecting $(d-1)$-dimensional "wall." It has been discovered that if the initial distance between the centers of the islands 2ℓ is large enough compared to their characteristic initial size and initial ratio of island to sea concentrations is relatively large, the evolution dynamics of the island-sea-island system is determined unambiguously by the dimensionless parameter

$$\Lambda = \mathcal{N}_0/\mathcal{N}_\Omega,$$

where $\mathcal{N}_0$ is the initial particle number in the island and $\mathcal{N}_\Omega$ is the initial number of sea particles in the volume $\Omega = (2\ell)^d$. It has been shown that:

(i) In the limit of small $\Lambda^{2/d} \ll 1$ each of the islands evolves and dies *autonomously* not feeling the presence of neighboring island;

(ii) There is a threshold value

$$\Lambda_\star = (\pi e/2d)^{d/2}/2,$$

below which the islands dies individually and above which island coalescence occurs;

(iii) Regardless of d the centers of each of the islands move toward each other along the universal trajectory, merging in a united center at the critical value

$$\Lambda_s = (\sqrt{e}/2)(\pi/2)^{d/2} \geqslant \Lambda_\star,$$

so that at $\Lambda > \Lambda_s$ coalescence is completed by the collapse of the single-centered island in the system center;

(iv) In 2D and 3D systems in the range $\Lambda_\star < \Lambda < \Lambda_s$ the coalescence is accompanied by the subsequent fragmentation (division) of the two-centered island and is completed by individual collapse of each of the islands.

In Ref. [36] a detailed picture of coalescence, fragmentation, and collapse of the *identical* islands is presented, the remarkable properties of self-similarity of the evolution of islands are revealed, and a comprehensive self-consistent picture of the relative front width evolution is given. Generalizing the model developed in Ref. [36], in this article we consider a much more complex and nontrivial problem of diffusion-controlled interaction and collapse of two *nonidentical* spatially separated A-particle islands submerged in the B-particle sea. We show that at a sufficiently large initial distance between the centers of islands 2ℓ and a relatively large initial ratio of island to sea concentrations, the evolution dynamics of the island-sea-island system demonstrates remarkable universality and is determined unambiguously by two dimensionless parameters,

$$\Lambda = \mathcal{N}_0^+/\mathcal{N}_\Omega$$

and

$$q = \mathcal{N}_0^-/\mathcal{N}_0^+,$$

where $\mathcal{N}_0^+$ and $\mathcal{N}_0^-$ are the initial particle numbers in the larger and smaller of the islands, respectively, and $\mathcal{N}_\Omega$ is the initial number of sea particles in the volume $\Omega = (2\ell)^d$. We find that at each fixed $0 < q \leqslant 1$, there are threshold values $\Lambda_\star(q)$ and $\Lambda_s(q) \geqslant \Lambda_\star(q)$ that depend on the dimension and separate the domains of individual death of the islands $\Lambda < \Lambda_\star(q)$, coalescence and subsequent fragmentation of a two-centered island $\Lambda_\star(q) < \Lambda < \Lambda_s(q)$, and collapse of a single-centered island formed by coalescence $\Lambda > \Lambda_s(q)$. We demonstrate that regardless of d, the trajectories of the island centers are determined unambiguously by the parameter q, and we reveal a detailed picture of the evolution of islands and front trajectories with an increase in Λ, focusing on the scaling laws of evolution in the vicinity of coalescence, fragmentation, and collapse points. Finally, we give a comprehensive analysis of the relative front width evolution and show that the presented picture of island evolution is self-consistent in a wide range of parameters.

II. DIFFUSION-CONTROLLED INTERACTION OF NONIDENTICAL A-PARTICLE ISLANDS SUBMERGED IN THE B-PARTICLE SEA

A. Model

Let two nonidentical A-particle islands, which for simplicity have the shape of a d-dimensional hypercube with the side $2h$ and the centers of which are located on the x axis at the points $x = \pm \ell$, are surrounded by a uniform unlimited B-particle sea with the initial concentration b_0. We shall assume that initially in each of the islands A particles are distributed uniformly with the concentrations a_0^+ at the $x = +\ell$ center and $a_0^- \leqslant a_0^+$ at the $x = -\ell$ center, respectively. We shall also assume that initially the $\pm$ islands have the same spatial orientation and that the coordinate axes with the origin at the point $x = 0$ on the x axis are normal to hypercube "faces" so that $y \leftrightarrow -y, z \leftrightarrow -z$ symmetry takes place. Particles A and B diffuse with the diffusion constants $D_{A,B}$, and when meeting they annihilate with some nonzero probability $A + B \to 0$. In the continuum version, this process can be described by the reaction-diffusion equations

$$\partial a/\partial t = D_A \nabla^2 a - R, \quad \partial b/\partial t = D_B \nabla^2 b - R, \quad (2)$$

where $a(\mathbf{r}, t)$ and $b(\mathbf{r}, t)$ are the mean local concentrations of A and B and $R(\mathbf{r}, t)$ is the macroscopic reaction rate. We shall assume, as usual, that species diffusivities are equal $D_A = D_B = D$. This important condition, due to local conservation of difference concentration $a - b$, leads to a radical simplification that permits to obtain an analytical solution for arbitrary front trajectory [36]. Then, by measuring the length, time and concentration in units of $h, h^2/D$, and b_0, respectively, and defining the ratio $a_0^+/b_0 = c_+$, the ratio $a_0^-/b_0 = c_-$ and the ratio $L = \ell/h \gg 1$, we come from Eq. (2) to the simple diffusion equation for the difference concentration $s(\mathbf{r}, t) = a(\mathbf{r}, t) - b(\mathbf{r}, t)$,

$$\partial s/\partial t = \nabla^2 s, \quad (3)$$

at the initial conditions

$$s_0[x \in (L - 1, L + 1)] = c_+,$$
$$s_0[x \in -(L + 1, L - 1)] = c_-, \quad (4)$$

and $s_0 = -1$ (sea) outside the islands in the 1D case,

$$s_0[x \in (L - 1, L + 1), y \in (-1, +1)] = c_+,$$
$$s_0[x \in -(L + 1, L - 1), y \in (-1, +1)] = c_-, \quad (5)$$

and $s_0 = -1$ (sea) outside the islands in the 2D case,

$$s_0[x \in (L - 1, L + 1), y, z \in (-1, +1)] = c_+,$$
$$s_0[x \in -(L + 1, L - 1), y, z \in (-1, +1)] = c_-, \quad (6)$$

and $s_0 = -1$ (sea) outside the islands in the 3D case, with the boundary conditions

$$s(|\mathbf{r}| \to \infty, t) = -1 \quad (7)$$

and the symmetry conditions

$$\partial_y s \mid_{y=0} = \partial_z s \mid_{z=0} = 0.$$

Exact solution of the problem Eqs. (3)–(7) has the form

$$s(x, t) + 1 = \Gamma(x, t) = \frac{(c_+ + 1)}{2} \mathcal{L}_+ + \frac{(c_- + 1)}{2} \mathcal{L}_- \quad (8)$$

in the 1D case,

$$s(\mathbf{r}, t) + 1 = \Gamma(x, t) Q(y, t) \quad (9)$$

in the 2D case, and

$$s(\mathbf{r}, t) + 1 = \Gamma(x, t) Q(y, t) Q(z, t) \quad (10)$$

in the 3D case, where

$$\mathcal{L}_+(x, t) = \mathrm{erf}\left(\frac{L + 1 - x}{2\sqrt{t}}\right) - \mathrm{erf}\left(\frac{L - 1 - x}{2\sqrt{t}}\right), \quad (11)$$

$$\mathcal{L}_-(x, t) = \mathrm{erf}\left(\frac{L + 1 + x}{2\sqrt{t}}\right) - \mathrm{erf}\left(\frac{L - 1 + x}{2\sqrt{t}}\right), \quad (12)$$

and

$$Q(v, t) = \frac{1}{2}\left[\mathrm{erf}\left(\frac{1 + v}{2\sqrt{t}}\right) + \mathrm{erf}\left(\frac{1 - v}{2\sqrt{t}}\right)\right]. \quad (13)$$

According to the QSA in the diffusion-controlled limit at large $k \to \infty$ at times $t \propto k^{-1} \to 0$, there forms a sharp reaction front $w/|\mathbf{r}_f| \to 0$ so that in neglect of the reaction front width the solution $s(\mathbf{r}, t)$ defines the the law of its propagation

$$s(\mathbf{r}_f, t) = 0$$

and the evolution of particles distributions $a(\mathbf{r}, t) = s(\mathbf{r}, t) > 0$ within the island and $b(\mathbf{r}, t) = |s(\mathbf{r}, t) < 0|$ beyond it.

B. Long-time asymptotics in the sharp-front limit

We shall assume that the ratio of island to sea concentrations is large enough $c_+ \geqslant c_- \gg 1$ (concentrated islands). In Ref. [36], it has been shown that in the limit of large $c_+ = c_- = c \gg 1$ the "lifetime" of the islands $t_c \gg 1$, so the majority of the A particles die at times $t \gg 1$, when the diffusive length exceeds appreciably the initial island size. The evolution of the islands in such a large-t regime is of principal interest since, as it has been demonstrated in Ref. [36], in the limit of large $t \gg 1, L \gg 1$, and $c \gg 1$ regardless of the initial shape, orientation, and sizes of the islands the asymptotics of island evolution takes a universal form which at a given initial sea density is determined unambiguously only by the initial number of particles in the islands (the instantaneous source regime) and the initial distance between their centers. Assuming that the diffusion length $\sqrt{t} \gg 1$ and expanding the functions $\mathcal{L}_+(x, t)$, $\mathcal{L}_-(x, t)$, and $Q(v, t)$ in powers of $1/\sqrt{t}$ we find

$$\mathcal{L}_+(x, t) = \frac{2e^{-(L-x)^2/4t}}{\sqrt{\pi t}}(1 + \alpha_+), \quad (14)$$

$$\mathcal{L}_-(x, t) = \frac{2e^{-(L+x)^2/4t}}{\sqrt{\pi t}}(1 + \alpha_-), \quad (15)$$

$$Q(v, t) = \frac{e^{-v^2/4t}}{\sqrt{\pi t}}\left(1 - \frac{(1 - v^2/2t)}{12t} + \cdots\right), \quad (16)$$

where

$$\alpha_\pm = \frac{1}{12t}\left[\frac{(L \mp x)^2}{2t} - 1\right] + \cdots.$$

Neglecting further the transient terms $\alpha_{\pm}, (v/t)^2 \ll 1$, we conclude from Eqs. (8)–(10), (14)–(16) that in agreement with Refs. [31,36] regardless of the initial island shape (hypercube or hypersphere) at $1 \ll t \ll L^2$ each of the $\pm$ islands takes the shape of a d-dimensional sphere with the front radius $\rho_f^{\pm}(t)$ which changes by the law

$$\rho_f^{\pm}(t) = \sqrt{2dt \ln(t_c^{\pm}/t)}, \tag{17}$$

whence it follows that at any d in the limit of large $1 \ll c_{\pm} \ll L^d$ each of the $\pm$ islands first expands reaching some maximal radius $\rho_f^{M,\pm}$, and then it contracts disappearing in the collapse point

$$t_c^{\pm} = \frac{(c_{\pm}+1)^{2/d}}{\pi} = \frac{(\gamma_{\pm} N_0^{\pm})^{2/d}}{4\pi}, \tag{18}$$

where $\gamma_{\pm} = (c_{\pm}+1)/c_{\pm} \approx 1$ and $N_0^{\pm}$ is the initial particle number in the island in units of $h^d b_0$.

C. Instantaneous source regime

According to Eqs. (14)–(17), at large $L \gg 1$ in the domain $t \gg \mathsf{Max}[1, \ln(t_c^{\pm}/t)]$ evolution of each of the $\pm$ islands bounded by the front becomes independent on its initial size, therefore, the initial distance between the island centers 2ℓ becomes the only length scale determining the evolution. Then by measuring the length and time in units of ℓ and ℓ^2/D, i.e., going to the dimensionless variables $T = t/L^2, X = x/L, Y = y/L, Z = z/L$, and neglecting the transient terms $\alpha_{\pm}, (v/t)^2 \ll 1$ we find from Eqs. (8)–(10), (14)–(16),

$$s + 1 = \frac{\Lambda}{(\pi T)^{d/2}} \exp\left[-\frac{(1-X)^2 + \varrho^2}{4T}\right](1 + qe^{-X/T}), \tag{19}$$

where $\Lambda = (c_+ + 1)/L^d$, $q = (c_- + 1)/(c_+ + 1)$ and $\varrho^2 = Y^2$ or $\varrho^2 = Y^2 + Z^2$ at $d = 2, 3$, respectively. We conclude from Eq. (19) that in the instantaneous source regime evolution dynamics of the asymmetrical island-sea-island system is determined unambiguously by two dimensionless parameters,

$$\Lambda = \mathcal{N}_0^+ / \mathcal{N}_\Omega$$

and

$$q = \mathcal{N}_0^- / \mathcal{N}_0^+,$$

where in view of the requirement $c_{\pm} \gg 1(\gamma_{\pm} \approx 1)$ $\mathcal{N}_0^+$ and $\mathcal{N}_0^-$ are the initial particle numbers in larger (+) and smaller (−) of the islands, respectively, and $\mathcal{N}_\Omega$ is the initial number of sea particles in the volume $\Omega = (2\ell)^d$. Taking $s_f = 0$ we derive from Eq. (19) the law of the reaction front motion

$$\exp\left(-\frac{(1-X_f)^2 + \varrho_f^2}{4T}\right)(1 + qe^{-X_f/T}) = \frac{(\pi T)^{d/2}}{\Lambda}. \tag{20}$$

Equations (19) and (20) are basic equations that determine the evolution of the islands and front trajectories for an arbitrary ratio of the initial number of particles in the islands $0 < q \leqslant 1$, including the evolution of identical islands considered in Ref. [36] as the special particular case $q = 1$. Our goal will be to reveal the key regularities of the interaction and evolution of the islands and fronts in the instantaneous source regime.

III. EVOLUTION OF THE ASYMMETRICAL ISLAND-SEA-ISLAND SYSTEM IN THE INSTANTANEOUS SOURCE REGIME: COALESCENCE, FRAGMENTATION, AND COLLAPSE OF ISLANDS

A. Trajectories of the centers of islands and sea: Thresholds of coalescence $\Lambda_{\star}(q)$ and of a single-centered island formation $\Lambda_s(q)$

It follows from Eq. (19) that, as well as in the special particular case of identical islands, at any d the points where the concentration of A particles reaches its maximum, which we will call the island centers, are located on the X axis. Calculating the trajectories of motion of the centers $X_{\star}(T)$ from the condition $\partial s/\partial X = 0$, we find from Eq. (19)

$$\frac{1 - X_{\star}}{1 + X_{\star}} = qe^{-X_{\star}/T}. \tag{21}$$

In the general case, Eq. (21) has three real roots: $X_{\star}^{(+)}, X_{\star}^{(-)}$, and $X_{\star}^{(0)}$. The first two roots describe the trajectories of the centers of the $\pm$ islands,

$$0 \leqslant X_{\star}^{(+)}(q, T) \leqslant 1$$

and

$$-1 \leqslant X_{\star}^{(-)}(q, T) < 0,$$

respectively. The third root, $X_{\star}^{(0)}(q, T)$, which we will call the sea center, determines the trajectory of the local minimum of s:

$$X_{\star}^{(-)}(q, T) < X_{\star}^{(0)}(q, T) \leqslant 0.$$

It is important to emphasize that, regardless of d and Λ, the trajectories of the centers are the single-valued functions of the parameter q. In the limit of small $T \ll 1$, from Eq. (21) we find

$$\begin{aligned}X_{\star}^{(+)}(q, T) &= 1 - 2qe^{-1/T} + \cdots, \\ X_{\star}^{(-)}(q, T) &= -1 + (2/q)e^{-1/T} + \cdots, \\ X_{\star}^{(0)}(q, T) &= T \ln q + \cdots,\end{aligned} \tag{22}$$

whereas in the limit of large $T \gg 1$, we derive

$$X_{\star}^{(+)}(q, T) = \frac{(1-q)}{(1+q)}(1 + \alpha_q/T + \cdots), \tag{23}$$

where $\alpha_q = 2q/(1 + q)$. The trajectories of the islands and sea centers calculated according to Eq. (21) for several fixed values of q are shown in Fig. 1. One can see that at $q < 1$, according to Eqs. (22), with an increase in T the centers of the smaller island, $X_{\star}^{(-)}(T)$, and sea, $X_{\star}^{(0)}(T)$, move toward each other with acceleration, merging in a united center at some critical point $[T_s(q), X_s(q)]$ that obviously is the inflection point, as shown by the arrows below:

$$\mathsf{Max}_X(s) \to \frac{\partial^2 s}{\partial X^2}[T_s, X_s] = 0 \leftarrow \mathsf{Min}_X(s).$$

Determining the trajectory of the inflection point $X_s(T)$ from Eq. (19), we find
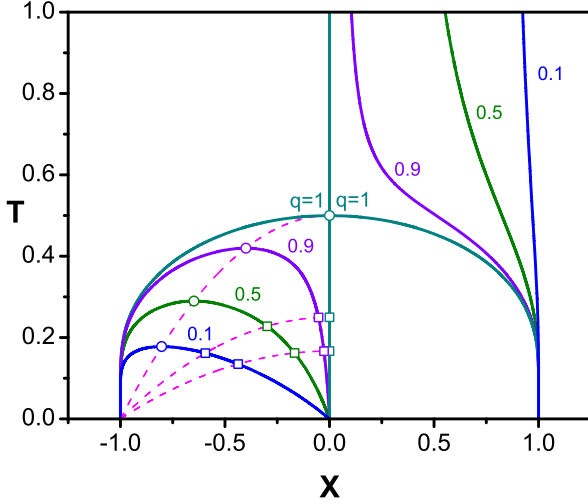
$$X_s^2 = 1 - 2T,$$

FIG. 1. The trajectories of the center of the smaller island $-1 \leqslant X_\star^{(-)}(q, T) < X_s(q)$, the center of the sea $X_s(q) < X_\star^{(0)}(q, T) \leqslant 0$, and the center of the larger island $0 \leqslant X_\star^{(+)}(q, T) \leqslant 1$ calculated from Eq. (21) for $q = 1, 0.9, 0.5$ and 0.1. Dashed lines show the trajectories $X_M(T) = -(1 - 2dT)^{1/2}$ for $d = 1, 2$, and 3 (from top to bottom). Squares and circles mark the critical points X_M, T_M and X_s, T_s, respectively (note that at $d = 1$, $X_M = X_s$ and $T_M = T_s$).

whence, in combination with Eq. (21), it follows that for each fixed value of q, regardless of d the coordinates of the critical point $T_s(q), X_s(q)$ are unambiguously fixed by the system of equations

$$\frac{1 - X_s}{1 + X_s} = qe^{-X_s/T_s}, \quad T_s = \frac{\left(1 - X_s^2\right)}{2}. \quad (24)$$

One can see from Fig. 1 that at the critical point $T_s(q), X_s(q)$, the center of the smaller island $X_\star^{(-)}$ "disappears." It follows from this that the collapse of the smaller island on the trajectory $X_\star^{(-)}(T)$ occurs only at $T < T_s(q)$, whereas at $T > T_s(q)$ a single-centered island is formed as a result of islands coalescence, the collapse of which occurs on the trajectory $X_\star^{(+)}(T)$. According to Eqs. (21) and (24), at $q < 1$ the trajectories of the centers of the smaller island and sea reach the critical point $T_s(q), X_s(q)$ by the universal law

$$|X_s - X_\star| = \sqrt{2(T_s - T)} + \cdots . $$

In the special particular case of identical islands $q = 1$ with mirror $-X \leftrightarrow X$ symmetry, the centers of both islands $X_\star^{(+)}(1, T) = |X_\star^{(-)}(1, T)|$ merge in a united center with the stationary sea center $X_\star^{(0)}(1, T) = 0$ at the critical point $T_s(1) = 1/2$, above which the formed single-centered island dies in the system center $X_\star(1, T > 1/2) = 0$, by the law $|X_\star^{(\pm)}| = \sqrt{6(T_s(1) - T)} + \cdots$ [36].

Assuming that $s_\star^{(-)}(T_s, X_s) = 0$, from Eqs. (19) and (24) we find the threshold of single-centered island formation

$$\Lambda_s(q) = (\pi T_s)^{d/2}(1 + X_s)\exp[(1 - X_s)^2/4T_s]/2, \quad (25)$$

below which each of the islands dies in its own center. It is easy to demonstrate from Eqs. (19) and (21) that in the domain $\Lambda \leqslant \Lambda_s(q)$ on the trajectory of the sea center $X_\star^{(0)}(q, T)$ the quantity $s_\star^{(0)}$ passes through the maximum $s_\star^{(0)}(T_M, X_M) = \mathsf{Max}[s_\star^{(0)}(T)]$ at some point $T_M(q), X_M(q)$. Determining the

trajectory of point of the maximum $X_M(T)$ from the condition $ds_\star/dT = 0$, we find from Eqs. (19) and (21)

$$X_M^2 = 1 - 2dT,$$

whence, in combination with Eq. (21), it follows that for each fixed value of q, depending on the system dimension d, the coordinates of the maximum point $T_M(q), X_M(q)$ are unambiguously fixed by the system of equations (Fig. 1)

$$\frac{1 - X_M}{1 + X_M} = qe^{-X_M/T_M}, \quad T_M = \frac{\left(1 - X_M^2\right)}{2d}. \quad (26)$$

It is easy to show that at a fixed value of q, with an increase in Λ the quantity $s_\star^{(0)}(T_M, X_M)$ increases passing through 0 at some threshold value $\Lambda_\star(q)$. Assuming that $s_\star^{(0)}(T_M, X_M) = 0$ (the condition $s_\star^{(0)} = 0$ obviously determines the point of contact of the $\pm$-islands fronts, see below), we find from Eqs. (19) and (26) the threshold of islands coalescence in the form

$$\Lambda_\star(q) = (\pi T_M)^{d/2}(1 + X_M)\exp[(1 - X_M)^2/4T_M]/2. \quad (27)$$

It follows from Eqs. (24)–(27) that at any q, the regularities of the island-sea-island system evolution *differ qualitatively* at $d = 1$ and $d > 1$.

In 1D systems $\Lambda_\star(q) = \Lambda_s(q)$, $T_M(q) = T_s(q)$, $X_M(q) = X_s(q)$, that is why in the domain $\Lambda < \Lambda_\star(q)$ each of the islands dies *individually*, not touching the partner, whereas above the threshold $\Lambda > \Lambda_\star(q)$ the single-centered island formed during coalescence dies on the trajectory $X_\star^{(+)}(T > T_s)$.

At $d > 1$ in the range $\Lambda_\star(q) < \Lambda < \Lambda_s(q)$ the function $s_\star^{(0)}(T, X_\star)$ obviously passes through two zeros, the first of which, $s_\star^{(0)}(T_{cl}, X_{cl}) = 0$, determines the starting point of islands coalescence

$$T_{cl}(q, \Lambda) < T_M(q), \quad X_{cl}(q, \Lambda) > X_M(q),$$

whereas the second one, $s_\star^{(0)}(T_{fr}, X_{fr}) = 0$, determines the starting point of the fragmentation (division) of the formed two-centered (dumbbell-like) island

$$T_{fr}(q, \Lambda) > T_M(q), \quad X_{fr}(q, \Lambda) < X_M(q),$$

which again splits into two separated islands with subsequent death in the corresponding centers $X_\star^{(\pm)}$. In the domain $\Lambda > \Lambda_s(q)$, only the first of these zeros "remains," which, as well as in the 1D case, determines the starting point of islands coalescence that forms a single-centered island dying on the trajectory $X_\star^{(+)}(T > T_s)$. As in the special mirror-symmetrical case of identical islands, $q = 1$ [36], it is easy to understand the reasons for absence of intermediate coalescence-fragmentation domain in 1D systems. Indeed, in 2D and 3D systems, the sea always remains topologically continuous (pathwise connected), that is why after the formation of an isthmus between the islands (coalescence) the current of sea particles normal to the X axis strives to destroy the isthmus ($A + B \to 0$) and achieves this (fragmentation) in the range $\Lambda_\star(q) < \Lambda < \Lambda_s(q)$ as the islands are depleted. In a qualitative contrast to that, in 1D systems the sea consists of two areas separated by the islands: a finite "internal" sea area enclosed between the fronts and an unbounded "external" sea. Thus, after disappearance of the internal sea area (coalescence) collapse of the formed island is the only remaining outcome of the reaction in 1D systems.
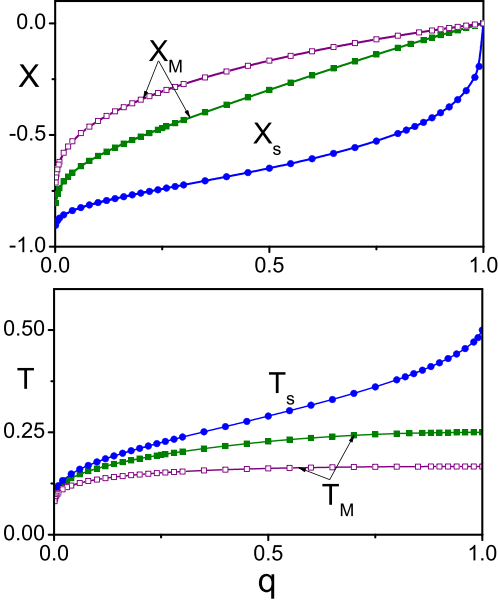
FIG. 2. Dependencies $X_s(q)$, $T_s(q)$ (circles) and $X_M(q)$, $T_M(q)$ (squares) calculated from Eqs. (24) and (26) for $d = 1$ (circles), $d = 2$ (filled squares), and $d = 3$ (open squares).

Thus, we conclude that at each fixed $0 < q \leqslant 1$ there are threshold values $\Lambda_\star(q)$ and $\Lambda_s(q) \geqslant \Lambda_\star(q)$ that depend on the dimension and separate domains of the individual death of the islands $\Lambda < \Lambda_\star(q)$, coalescence and subsequent fragmentation of the islands $\Lambda_\star(q) < \Lambda < \Lambda_s(q)$, and collapse of the single-centered island formed by coalescence $\Lambda > \Lambda_s(q)$. Figures 2 and 3 demonstrate dependencies of the critical points of the thresholds of coalescence $T_M(q)$, $X_M(q)$, $\Lambda_\star(q)$ and of formation of the single-centered island $T_s(q)$, $X_s(q)$, $\Lambda_s(q)$ on the ratio of the initial numbers of particles in the islands q, calculated according to Eqs. (24)–(27) for $d = 1, 2$, and 3. One can see from Fig. 2 that, according to Fig. 1, with a decrease in q, the coordinates $X_M(q)$ and $X_s(q)$ shift toward the initial center of the smaller island as a consequence of the acceleration of motion of the sea center caused by the deceleration of expansion of the smaller island [$X_M(q), X_s(q) \to -1$ as $q \to 0$]. Correspondingly, the duration of the periods $T_M(q)$ and $T_s(q)$ decreases with a decrease in q [$T_M(q), T_s(q) \propto 1/|\ln q| \to 0$ as $q \to 0$]. It is worth noticing, however, that in 3D systems the period $T_M(q)$ remains almost constant in a wide range of q. It should be also emphasized that even a slight difference in the initial numbers of particles in the islands $1 - q \ll 1$ results in a significant shift of the coordinate $X_s(q)$: $X_s(q) \sim -(1 - q)^{1/3} + \cdots$. Figure 3 demonstrate that with a decrease in q, the thresholds of coalescence $\Lambda_\star(q)$ and of the single-centered island formation $\Lambda_s(q)$ increase rapidly [except for a slight initial decrease in $\Lambda_s(q)$ at $d = 3$] with the higher velocity, the lower q

$$\Lambda_\star(q), \Lambda_s(q) \propto 1/q|\ln q|^{d/2} \to \infty$$

as $q \to 0$. One of the important consequences of Fig. 3 is that with a decrease in q, the relative width of the fragmentation domain ($d = 2, 3$) contracts relatively rapidly, as demonstrated by the insets.
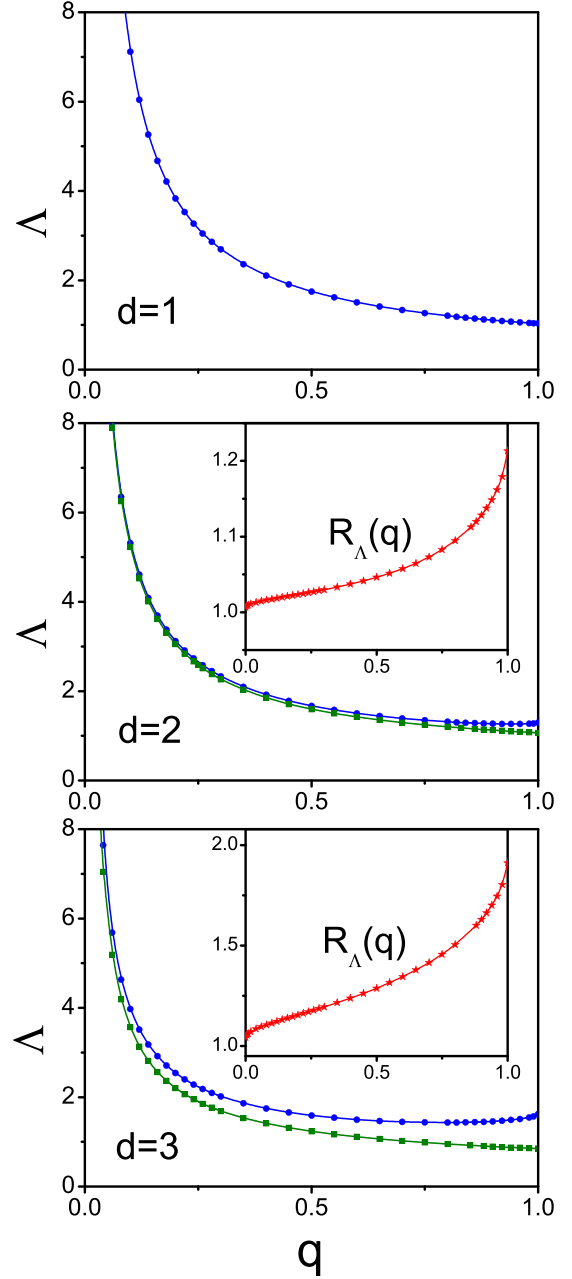

FIG. 3. Dependencies $\Lambda_s(q)$ (circles) and $\Lambda_\star(q)$ (squares) calculated from Eqs. (25) and (27) for $d = 1, 2$, and 3 [note that at $d = 1 \Lambda_\star(q) = \Lambda_s(q)$]. Insets: Dependencies $R_\Lambda(q) = \Lambda_s(q)/\Lambda_\star(q)$.

B. Front trajectories: Coalescence, fragmentation, and collapse of islands

1. Evolution of front trajectories with an increase in Λ

According to Eq. (20), in the domain of individual death of the islands $\Lambda < \Lambda_\star$, each of the $\pm$ islands with the centers $X_\star^{(+)}(q, T)$ and $X_\star^{(-)}(q, T)$, respectively, is limited on the X axis by two leading front points (by two fronts in the 1D case) $X_{f,<}^{(\pm)} \leqslant X_\star^{(\pm)}$ and $X_{f,>}^{(\pm)} \geqslant X_\star^{(\pm)}$, which determine the width of each of the islands:

$$X_{f,<}^{(+)} \leqslant X_{isl}^{(+)} \leqslant X_{f,>}^{(+)}, \quad X_{f,<}^{(-)} \leqslant X_{isl}^{(-)} \leqslant X_{f,>}^{(-)}.$$

After the initial expansion and subsequent contraction of each of the islands, the leading front points merge in the corresponding collapse centers

$$\longrightarrow X_{f,<}^{(+)}(T_c^{(+)}) = X_\star^{(+)}(T_c^{(+)}) = X_{f,>}^{(+)}(T_c^{(+)}) \longleftarrow,$$

$$\longrightarrow X_{f,<}^{(-)}(T_c^{(-)}) = X_\star^{(-)}(T_c^{(-)}) = X_{f,>}^{(-)}(T_c^{(-)}) \longleftarrow,$$

the coordinates of which $T_c^{(+)}(q,\Lambda), X_c^{(+)}(q,\Lambda)$ and $T_c^{(-)}(q,\Lambda), X_c^{(-)}(q,\Lambda)$ are unambiguously fixed by the system of Eqs. (20) and (21) (here and below, the arrows show the directions of motion of the fronts toward the collapse and coalescence centers and away from the fragmentation centers). With an increase in the initial number of particles in the islands Λ, the amplitudes of island expansion at the front turning points increase rapidly. As a consequence, in the domain $\Lambda > \Lambda_\star$, the leading points of the neighboring fronts $X_{f,>}^{(-)}$ and $X_{f,<}^{(+)}$ merge and disappear (coalescence) at some time moment $T_{cl}(q,\Lambda)$

$$\longrightarrow X_{f,>}^{(-)}(T_{cl}) = X_\star^{(0)}(T_{cl}) = X_{f,<}^{(+)}(T_{cl}) \longleftarrow$$

forming either a single-centered ($\Lambda > \Lambda_s$) or two-centered (dumbbell-like) ($d = 2, 3, \Lambda_\star < \Lambda < \Lambda_s$) island. In 2D and 3D systems, in the range $\Lambda_\star < \Lambda < \Lambda_s$ the disappeared trajectories of the neighboring fronts $X_{f,>}^{(-)}$ and $X_{f,<}^{(+)}$ revive again at some moment of fragmentation start $T_{fr}(q,\Lambda)$

$$\longleftarrow X_{f,>}^{(-)}(T_{fr}) = X_\star^{(0)}(T_{fr}) = X_{f,<}^{(+)}(T_{fr}) \longrightarrow$$

disappearing in the corresponding collapse centers of each of the islands. As well as in the case of island collapse, the coordinates of the starting points of coalescence $T_{cl}(q,\Lambda), X_{cl}(q,\Lambda)$ and fragmentation $T_{fr}(q,\Lambda), X_{fr}(q,\Lambda)$ are unambiguously fixed by the system of Eqs.(20) and (21). In the domain $\Lambda > \Lambda_s$, the formation of a single-centered island is accompanied by the transformation

$$X_{f,<}^{(-)}(T < T_s) \rightarrow X_{f,<}^{(+)}(T > T_s),$$

which is completed by merging of the trajectories of the fronts $X_{f,<}^{(+)}$ and $X_{f,>}^{(+)}$ of the single-centered island at the collapse point $T_c^{(+)}$. As an illustration, Fig. 4 shows the evolution of the trajectories of the leading front points $X_f(T)|_{\varrho_f=0}$ with an increase in Λ, calculated from Eq. (20) for $d = 1$ at $q = 0.8$ and for $d = 2, 3$ at $q = 0.5$. One can see from Fig. 4 that with an increase in Λ, the effective interaction between the fronts results in significant deformation of their trajectories, which above the coalescence threshold $\Lambda_\star$ is accompanied by turning of the trajectory $X_{f,>}^{(-)}$ toward the sea center and formation of a single-centered or two-centered island. Figure 4 clearly demonstrates that at $\Lambda \neq \Lambda_\star, \Lambda_s$, in the vicinity of coalescence, fragmentation, and collapse points the velocities of these processes increase unlimitedly. It will be rigorously shown below that at any d and q, including the special case of mirror symmetry, the self-acceleration of coalescence, fragmentation, and collapse occurs by the law

$$|V_f| \propto |\mathcal{T}|^{-1/2} \rightarrow \infty,$$

as $\mathcal{T} \rightarrow 0$ where $\mathcal{T} = (T_0 - T)/T_0$ and $T_0 = T_{cl}, T_{fr}$ or $T_c^\pm$, respectively. As expected, the most interesting behavior that differs qualitatively from the special case of mirror symmetry is demonstrated by the trajectories of the fronts $q < 1$ at the critical points $\Lambda_\star$ and Λ_s.
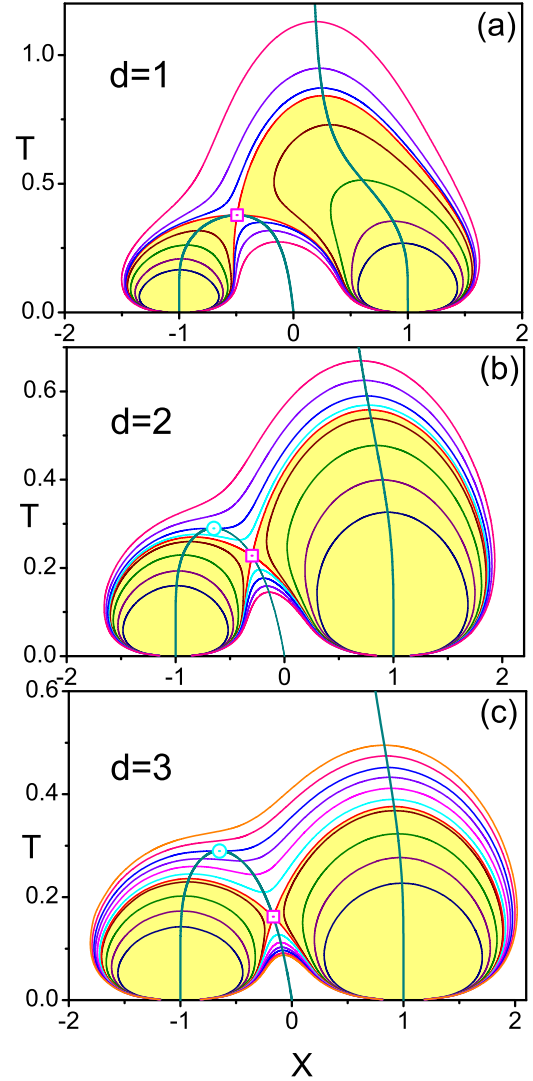

FIG. 4. Evolution of front trajectories with an increase in Λ. (a) 1D systems: The trajectories $X_{f,<}^{(\pm)}(T)$ and $X_{f,>}^{(\pm)}(T)$ calculated from Eq. (20) at $q = 0.8$ for $\Lambda = 0.9, 1, 1.1, 1.17, \Lambda_\star = 1.20562, 1.215, 1.24$, and 1.3; (b) 2D systems: The trajectories $X_{f,<}^{(\pm)}(T)$ and $X_{f,>}^{(\pm)}(T)$ calculated from Eq. (20) at $q = 0.5$ for $\Lambda = 1, 1.2, 1.4, 1.55, \Lambda_\star = 1.59556, 1.62, \Lambda_s = 1.66911, 1.75$, and 1.85; (c) 3D systems: The trajectories $X_{f,<}^{(\pm)}(T)$ and $X_{f,>}^{(\pm)}(T)$ calculated from Eq. (20) at $q = 0.5$ for $\Lambda = 0.6, 0.8, 1, 1.2, \Lambda_\star = 1.23657, 1.3, 1.4, 1.5, \Lambda_s = 1.59232, 1.7$, and 1.8. The growth of Λ corresponds to the visually observed growth of $T_c^{(-)}$ and $T_c^{(+)}$. The areas of individual collapse below the coalescence threshold are colored. Thick lines show the trajectories of the centers of the islands and the sea. Squares and circles mark the critical points X_M, T_M and X_s, T_s, respectively.

(i) *1D systems*. According to Fig. 4, in the 1D systems at the threshold value $\Lambda = \Lambda_\star = \Lambda_s$ three front trajectories $X_{f,<}^{(-)}(T), X_{f,>}^{(-)}(T)$, and $X_{f,<}^{(+)}(T)$ converge at the critical point X_M, T_M. One can see that in the vicinity of the critical point, the velocities of merging of the trajectories $X_{f,<}^{(-)}(T)$ and $X_{f,<}^{(+)}(T)$ increase unlimitedly

$$\left| V_{f,<}^{(-)}(T \rightarrow T_M) \right|, \quad \left| V_{f,<}^{(+)}(T \rightarrow T_M) \right| \rightarrow \infty,$$

whereas the trajectory $X_{f,>}^{(-)}(T)$ passes through the critical point with a finite velocity, transforming to the trajectory of a single-centered island $X_{f,<}^{(+)}(T)$, which disappears at the collapse point $T_c^{(+)} > T_M$

$$V_{f,>}^{(-)}(T = T_M - 0) = V_{f,<}^{(+)}(T = T_M + 0) = V_m^s(q).$$

It should be emphasized that at the threshold value $\Lambda = \Lambda_\star = \Lambda_s$ the smaller island and the "internal" area of the sea enclosed between the fronts die *simultaneously*.

(ii) *2D and 3D systems*. According to Fig. 4 in 2D and 3D systems at the threshold value $\Lambda = \Lambda_\star < \Lambda_s$ the trajectories of the neighboring fronts $X_{f,>}^{(-)}$ and $X_{f,<}^{(+)}$ converge at the critical point X_M, T_M with the finite velocities $V_{f,>}^{(-)}(T_M - 0) = V_m^M(q)$ and $V_{f,<}^{(+)}(T_M - 0) = V_p^M(q)$, respectively, "reflecting" at the time moment T_M in opposite directions with an instantaneous change of the velocity sign. It is remarkable that in the vicinity of the critical point of islands contact $T \to T_M$, front velocity along the "reflected" trajectory $V_{f,>}^{(-)}$ "inherits" front velocity along the incoming trajectory $V_{f,<}^{(+)}$

$$V_{f,>}^{(-)}(T_M + 0) = V_{f,<}^{(+)}(T_M - 0) = V_p^M(q),$$

whereas front velocity along the "reflected" trajectory $V_{f,<}^{(+)}$ "inherits" front velocity along the incoming trajectory $V_{f,>}^{(-)}$

$$V_{f,<}^{(+)}(T_M + 0) = V_{f,>}^{(-)}(T_M - 0) = V_m^M(q).$$

Figure 5 presents the dependencies $T_c^{(+)}(\Lambda)$, $T_c^{(-)}(\Lambda)$, $T_{cl}(\Lambda)$ and $T_{fr}(\Lambda)$ calculated from Eqs. (20) and (21) for $d = 1$ at $q = 0.8$ and for $d = 2, 3$ at $q = 0.5$. This dependencies together with Fig. 4 reveal a comprehensive picture of the location and extension of the domains of individual death of the islands, coalescence-fragmentation of the two-centered island with subsequent individual death of each of the islands, and coalescence-collapse of the single-centered island. The dependencies $T_{c,a}^{(+)} = (\Lambda)^{2/d}/\pi$ and $T_{c,a}^{(-)} = (q\Lambda)^{2/d}/\pi$ revealing the domains of the *autonomous* collapse of each of the islands $\Lambda^{2/d} \ll 1$ and $(q\Lambda)^{2/d} \ll 1$, respectively, are shown by dashed lines.

2. Critical value $q_\star$

According to Fig. 4 the critical point of islands contact T_M, X_M is the point of sudden turning of the larger island front, at which the front abruptly change the direction of its motion: up to this point, the larger island expands, and it begins to contract after islands contact ($V_m^M > 0$). Moreover, in 2D and 3D systems, the critical point of islands contact is the point of abrupt turning of the direction of motion of both fronts, up to which both islands expand and after the passage of which both islands begin to contract ($V_m^M > 0, V_p^M < 0$). It is clear, however, that with a decrease in the parameter q and a corresponding rapid increase in the coalescence threshold $\Lambda_\star(q)$ (Fig. 2), the expansion of the larger island after islands contact becomes the dominant trend. It will be rigorously demonstrated in the next section that there is a dimension-dependent critical value $q_\star(d)$ below which the velocity V_m^M changes its sign,

$$V_m^M(q > q_\star) > 0 \to V_m^M(q < q_\star) < 0,$$
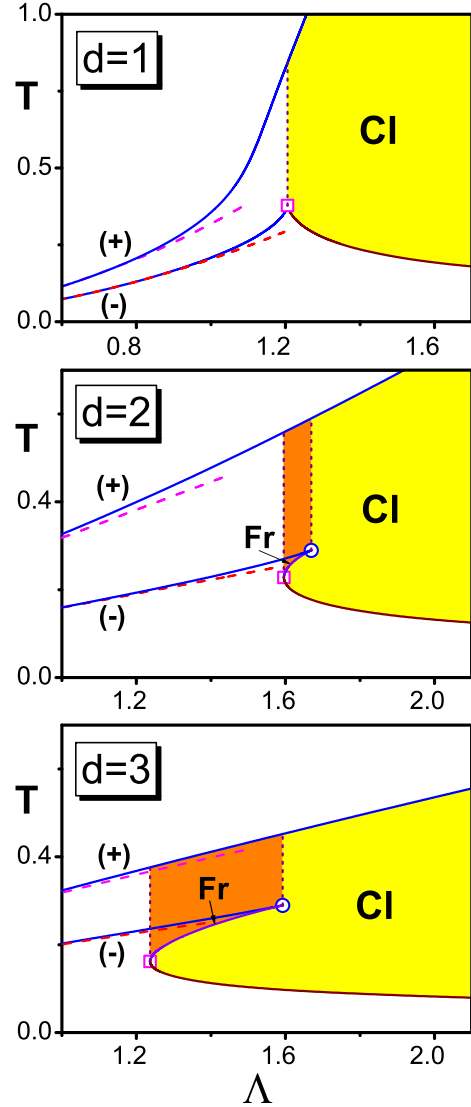

FIG. 5. Dependencies $T_c^{(-)}(\Lambda)$, $T_c^{(+)}(\Lambda)$, $T_{cl}(\Lambda)$, and $T_{fr}(\Lambda)$ calculated according to Eqs. (20) and (21) at $q = 0.8$ for $d = 1$ and at $q = 0.5$ for $d = 2, 3$ The areas of coalescence and fragmentation are colored. The critical points $\Lambda_\star, T_M$ and Λ_s, T_s are marked by squares and circles, respectively. The dashed lines show the asymptotics of the autonomous collapse.

and, consequently, the larger island continues to expand after the passage of the critical point T_M, X_M. It will be shown below that the condition $V_m^M(q_\star) = 0$ reduces to the requirement

$$T_M(q_\star) = X_M^2(q_\star) = \frac{1}{(2d + 1)}, \tag{28}$$

from which, according to Eq. (26), it follows that

$$q_\star(d) = \begin{cases} 0.660278..., & d = 1, \\ 0.279810..., & d = 2, \\ 0.157176..., & d = 3. \end{cases} \tag{29}$$

Figure 6 demonstrates evolution of the trajectories of leading front points $X_f(T)|_{\varrho_f=0}$ with an increase in Λ, calculated from Eq. (20) for $d = 1$ at $q = 0.5 < q_\star(1)$ and for $d = 2, 3$ at $q = 0.1 < q_\star(3) < q_\star(2)$. One can see that, in qualitative
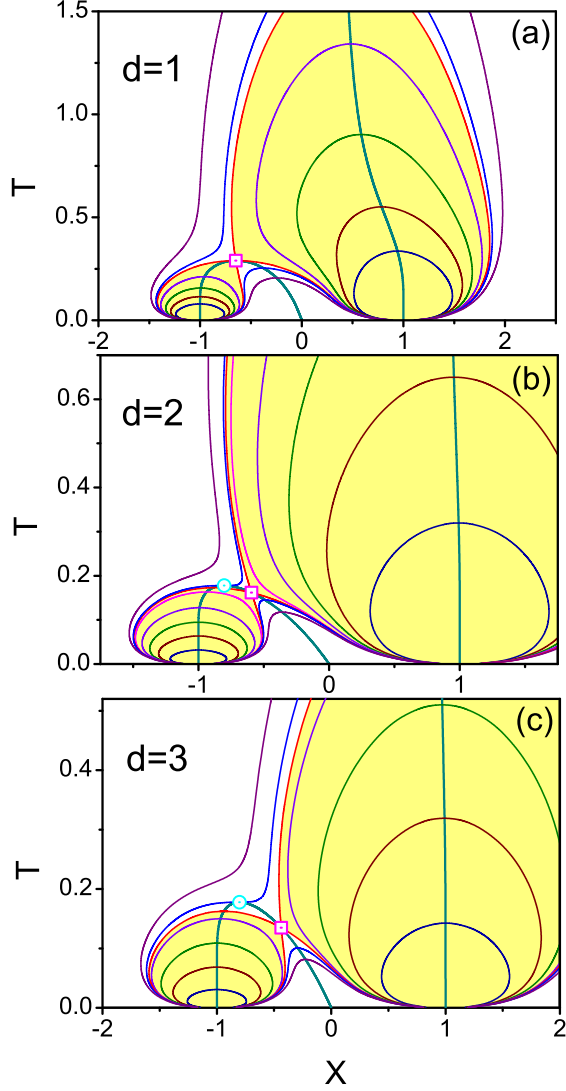
FIG. 6. Evolution of front trajectories with an increase in Λ at $q < q_\star(d)$. (a) 1D systems: The trajectories $X_{f,<}^{(\pm)}(T)$ and $X_{f,>}^{(\pm)}(T)$ calculated from Eq. (20) at $q = 0.5 < q_\star(1)$ for $\Lambda = 1, 1.2, 1.4, 1.6, \Lambda_\star = 1.74961, 1.8$, and 2; (b) 2D systems: The trajectories $X_{f,<}^{(\pm)}(T)$ and $X_{f,>}^{(\pm)}(T)$ calculated from Eq. (20) at $q = 0.1 < q_\star(2)$ for $\Lambda = 1, 2, 3, 4, 5, \Lambda_\star = 5.22736, \Lambda_s = 5.31766$, and 6; (c) 3D systems: The trajectories $X_{f,<}^{(\pm)}(T)$ and $X_{f,>}^{(\pm)}(T)$ calculated from Eq. (20) at $q = 0.1 < q_\star(3)$ for $\Lambda = 0.3, 1, 2, 3.2, \Lambda_\star = 3.56663, \Lambda_s = 3.97418$ and 5. The growth of Λ corresponds to the visually observed growth of $T_c^{(-)}$ and $T_c^{(+)}$. The areas of individual collapse below the coalescence threshold are colored. Thick lines show the trajectories of the centers of the islands and the sea. Squares and circles mark the critical points X_M, T_M and X_s, T_s, respectively.

contrast to the domain $q > q_\star$ where the fronts of the larger and smaller islands move to the contact point T_M, X_M toward each other ($V_{f,>}^{(-)} > 0, V_{f,<}^{(+)} < 0, T \to T_M$), in the domain $q < q_\star$ these fronts move in one direction ($V_{f,>}^{(-)} < 0, V_{f,<}^{(+)} < 0, T \to T_M$) realizing islands contact as a consequence of the difference between the velocities of their fronts (at the critical point of islands contact, the "fast" front $|V_{f,<}^{(+)}| > |V_{f,>}^{(-)}|$) "overtakes" the "slow" front). According to Fig. 6 in 1D systems, at the critical point of death of the smaller island T_M, X_M

the front of the larger island slows down abruptly, continuing to move in the same direction up to the front turning point, which shifts toward $T > T_M$. In 2D and 3D systems, at the critical point of islands contact T_M, X_M the fronts $X_{f,>}^{(-)}$ and $X_{f,<}^{(+)}$ abruptly exchange their velocities, continuing to move in one direction, and, as a consequence, their effective "attraction" change to effective "repulsion." Thus, after the passage of the contact point, the smaller island continues to contract up to the collapse point, while the larger island continues to expand up to the front turning point, which shifts toward $T > T_M$. It should be emphasized that in the domain $q < q_\star$, in the range $\Lambda_\star < \Lambda < \Lambda_u$ widening with a decrease in q, the competition between diffusion fluxes results in the emergence of two front turning points on the trajectory $X_{f,<}^{(+)}(T > T_M)$, as is clearly demonstrated in Fig. 6(b).

3. Universality of evolution in the system center

According to Eq. (19), in the system center $\mathbf{r} = 0$ we find

$$s(\mathbf{0}, T) + 1 = \frac{\Lambda(1 + q)}{(\pi T)^{d/2}} \exp(-1/4T), \quad (30)$$

from which a remarkable fact follows immediately that the evolution of particle concentration in the system center is determined unambiguously by only the reduced total initial number of A-particles in the islands $\Sigma = \Lambda(1 + q) = (\mathcal{N}_0^+ + \mathcal{N}_0^-)/\mathcal{N}_\Omega$ *regardless* of how these particles are distributed between the islands. From Eq. (28) we conclude that $s(\mathbf{0}, T)$ reach the maximum $s_M(\mathbf{0}) = \mathsf{Max}_T[s(\mathbf{0}, T)]$ at the time moment $T_M(\mathbf{0}) = 1/2d$ from which we obtain

$$s_M(\mathbf{0}) = \Sigma(2d/\pi e)^{d/2} - 1.$$

The condition $s_M(\mathbf{0}) = 0$ determines the threshold of the total initial number of particles in the islands,

$$\Sigma_\star = (\pi e/2d)^{d/2},$$

upon reaching which the leading point of the front of the larger island $X_{f,<}^{(+)}$ reaches the system center *regardless* of q. In the special case of mirror symmetry $q = 1$, the threshold $\Sigma_\star$ obviously fixes the threshold of islands coalescence $\Lambda_\star = \Sigma_\star/2$. In the domain $\Sigma > \Sigma_\star$ the condition $s(\mathbf{0}, T) = 0$ reveals two roots, $T_<(\mathbf{0}) < T_M(\mathbf{0})$ and $T_>(\mathbf{0}) > T_M(\mathbf{0})$. In the domain $q < 1$, the lower root, $T_<(\mathbf{0})$, determines the time of the first passage of the front $X_{f,<}^{(+)}$ through the system center and asymptotically decrease by the law $T_<(\mathbf{0}) \propto 1/\ln \Sigma$ with an increase in Σ, while the higher root $T_>(\mathbf{0})$ determines the time of the inverse passage of the front through the system center and asymptotically increase by the law $T_>(\mathbf{0}) \propto \Sigma^{2/d}$ with an increase in Σ. In the special case of mirror symmetry $q = 1$, the lower root determines the time of island coalescence start, while the higher root determines the time of fragmentation start ($\Lambda_\star < \Lambda < \Lambda_s$) or the collapse time of the single-centered island ($\Lambda > \Lambda_s$). Summing up, we conclude that although with a change in the initial ratio of particle numbers in the islands $q < 1$ the trajectories of fronts and island centers drastically change, *regardless* of q the times of the first and inverse passage of the leading point of the front $X_{f,<}^{(+)}$ through the system center are the universal functions of the total initial number of particles in the islands Σ, including the extreme case of complete absence of the smaller island

$q = 0$. The second remarkable fact that follows from Eq. (20) is that in 2D and 3D systems the evolution of the half-width (radius) of the island $\varrho_f(T)$ in the section $X = 0$ is determined unambiguously by the total initial number of particles in the islands,

$$\varrho_f(T) = \sqrt{2dT \ln(\Sigma^{2/d}/\pi T) - 1},$$

reaching the maximum,

$$\varrho_f^M = \sqrt{(\Sigma/\Sigma_\star)^{2/d} - 1},$$

at the time moment $T_M^\varrho = (\Sigma/\Sigma_\star)^{2/d}/2d$.

IV. EVOLUTION OF ISLANDS IN THE VICINITY OF COALESCENCE, FRAGMENTATION AND COLLAPSE POINTS

A. Self-similar evolution of islands at the final collapse stage

Let $\Delta = X - X_c$ and $\mathcal{T} = (T_c - T)/T_c$, where $X_c|_{\varrho=0}$, T_c are the coordinates of collapse points of the smaller $(X_c^{(-)}, T_c^{(-)})$ or larger $(X_c^{(+)}, T_c^{(+)})$ island on the trajectories of the centers $X_\star^{(-)}(T)$ and $X_\star^{(+)}(T)$, respectively. Then, in the limit of small $|\Delta| \ll 1$, $|\varrho| \ll 1$ and $|\mathcal{T}| \ll 1$ from Eqs. (19) and (21) we obtain expansion in powers of Δ, ϱ and $\mathcal{T}$ in the form

$$\frac{s - s_c}{1 + s_c} = \mathcal{F}(\Delta) + \mathcal{E}(\varrho)[1 + \mathcal{F}(\Delta)], \tag{31}$$

where the concentration of A-particles at the collapse point Δ, $\varrho = 0$ decreases by the law

$$s_c = \mathcal{T}(d - \chi_c)/2 + m_c \mathcal{T}^2 + \cdots,$$

$$m_c = \frac{(d + 2)}{8}(d - 2\chi_c) + \frac{\chi_c(1 + 3X_c^2)}{16T_c},$$

and expansions of the functions $\mathcal{F}(\Delta)$ and $\mathcal{E}(\varrho)$ in powers of Δ and ϱ, respectively, have the form

$$\mathcal{F}(\Delta) = c_1 \Delta + c_2 \Delta^2 + c_3 \Delta^3 + c_4 \Delta^4 + \cdots,$$

and

$$\mathcal{E}(\varrho) = -\varrho^2(1 + \mathcal{T} - \varrho^2/8T_c + \cdots)/4T_c + \ldots,$$

where the coefficients

$$c_1 = \frac{\chi_c X_c \mathcal{T}}{2T_c}[1 + \mathcal{O}(\mathcal{T}) + \cdots],$$

$$c_2 = -\frac{1 - \chi_c + \omega \mathcal{T} + \cdots}{4T_c},$$

$$\omega = 1 + \chi_c(X_c^2/T_c - 2),$$

$$c_3 = -\frac{\chi_c X_c}{12T_c^2}[1 + \mathcal{O}(\mathcal{T}) + \cdots],$$

$$c_4 = \frac{1 + \chi_c(X_c^2/2T_c + 1/6T_c - 2)}{32T_c^2}[1 + \mathcal{O}(\mathcal{T}) + \cdots],$$

and the notation is introduced,

$$\chi_c = \frac{(1 - X_c^2)}{2T_c}. \tag{32}$$

1. Self-similar collapse at the critical point $\Lambda_s = \Lambda_\star$ of 1D systems

At the critical point $\Lambda = \Lambda_\star = \Lambda_s$ we have $X_c^{(-)} = X_s$, $T_c^{(-)} = T_s$, whence, according to Eqs. (24) and (32) it follows that

$$\chi_c^{(-)} = \chi_s = 1,$$

and for $d = 1$ at small $|\mathcal{T}| \ll 1$ from Eq. (31) we find

$$s_c = m_s \mathcal{T}^2 + \cdots, \quad c_2 = -\omega \mathcal{T}/4T_s + \cdots.$$

Assuming further that $q < 1$, $|\Delta| \ll T_s|X_s|$, at small $|\mathcal{T}|$ we derive from Eq. (31) with accuracy to leading terms

$$s = m_s \mathcal{T}^2 + c_1 \Delta + c_3 \Delta^3 + \cdots, \tag{33}$$

whence, substituting here the condition $s_f = 0$, we find asymptotic trajectories of the fronts

$$\Delta_{f,<}^{(\pm)} = \pm\sqrt{6T_s\mathcal{T}} + \cdots,$$

$$\Delta_{f,>}^{(-)} = \left(\frac{2m_s T_s}{|X_s|}\right)\mathcal{T} + \cdots. \tag{34}$$

From Eq. (34), the result announced above follows immediately that the front $\Delta_{f,>}^{(-)}$ approaches the collapse point X_s with the finite velocity

$$V_m^s = d\Delta_{f,>}^{(-)}/dT|_{\mathcal{T}\to 0} = -2m_s/|X_s| + \cdots$$

maintaining it after the transformation $\Delta_{f,>}^{(-)}(T_s - 0) \to \Delta_{f,<}^{(+)}(T_s + 0)$. Moreover, according to Eq. (31), with a decrease in the parameter q, the coefficient m_s and, as a consequence, the velocity of the front V_m^M change their sign $m_s(q \to 1) < 0 \to m_s(q \to 0) > 0$, passing according to Eq. (28) through 0 at the critical value $q = q_\star$, where $T_s(q_\star) = X_s^2(q_\star) = 1/3$.

According to Eq. (33), up to the moment of smaller island collapse ($\mathcal{T} \to 0$), the distribution of particles in the smaller island and internal sea area can be presented in the form $s(\Delta, \mathcal{T}) = m_s \mathcal{T}^2 + \mathcal{T}^{3/2}\mathcal{S}(\Delta/\sqrt{\mathcal{T}})$, whence it follows that the dominant evolution of this distribution occurs on the time scale $\propto \mathcal{T}^{3/2}$. By neglecting on this scale the transient term $\propto \mathcal{T}^2$, we conclude that in 1D systems at the final collapse stage the distribution of particles in the smaller island and internal area of the sea takes the universal scaling form

$$s(\Delta, \mathcal{T}) = \mathcal{T}^{3/2}\mathcal{S}(\Delta/\sqrt{\mathcal{T}}), \tag{35}$$

where the scaling function $\mathcal{S}(\xi)$ is the odd function of ξ. Thus, in qualitative contrast to the mirror-symmetrical case $q = 1$ [36], where the distribution of particles of the island and internal sea area at the final collapse stage is described by the even scaling law $s(X, \mathcal{T}) = \mathcal{T}^2 F(X/\sqrt{\mathcal{T}})$ and, as a consequence, the distribution of particles in the island and sea differs significantly, in the domain $q < 1$ the distribution of particles in the smaller island and internal area of the sea asymptotically becomes the same with the same number of A- and B-particles in the island and sea, respectively. Moreover, it is remarkable that in the domain $q < 1$, at the final collapse stage the number of particles of the smaller island decreases much slower, $\propto \mathcal{T}^2$, than in the mirror-symmetrical case, $\propto \mathcal{T}^{5/2}$. As an illustration, Fig. 7 demonstrates collapse of the normalized distribution of particles $|s(\Delta/\mathcal{T}^{1/2})|/\mathcal{T}^{3/2}$
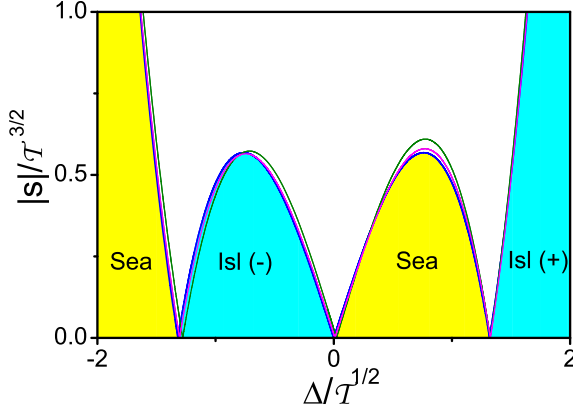
FIG. 7. Collapse of normalized distribution $|s(\Delta/\mathcal{T}^{1/2})|/\mathcal{T}^{3/2}$ to the scaling function Eq. (35) at $q = 0.5$ and $\Lambda = \Lambda_\star$. Thin lines—$\mathcal{T} = 0.05, 0.01$ Eq. (19); thick line—scaling function $|\mathcal{S}(\Delta/\mathcal{T}^{1/2})|$. Area under scaling function $|\mathcal{S}(\Delta/\mathcal{T}^{1/2})|$ is colored.

to the scaling function $|\mathcal{S}(\Delta/\mathcal{T}^{1/2})|$ as $\mathcal{T} \rightarrow 0$ at $q = 0.5$ and $\Lambda = \Lambda_\star$.

2. Final stage of evolution of two-centered island at the critical point Λ_s of 2D and 3D systems

In 2D and 3D systems at the critical point $\Lambda = \Lambda_s > \Lambda_\star$, as well as in the case of 1D systems, from Eqs. (24) and (32) we find

$$\chi_c^{(-)} = \chi_s = 1,$$

whence, according to Eq. (31), for $d > 1$ at small $|\mathcal{T}| \ll 1$ it follows that

$$s_c = (d - 1)\mathcal{T}/2 + \cdots, \quad c_2 = -\omega\mathcal{T}/4T_s + \cdots.$$

In radical contrast to 1D systems, where at the critical point $T_s = T_M$ the smaller island disappears at the moment of islands contact, in 2D and 3D systems long before disappearance of the smaller island center a united two-centered island is formed ($T_s > T_M$). Moreover, in qualitative contrast to the mirror-symmetrical case $q = 1$, where the collapse of the two-centered island occurs at the moment $T_c = T_s(1)$ [36], at $d > 1$ in the domain $q < 1$ at the moment $T = T_s(q)$ the united two-centered island becomes single-centered, continuing to evolve up to the point of its collapse $T_c^{(+)} > T_s$.

Assuming that $q < 1$ and $|\Delta| \ll T_s|X_s|$ at small $|\mathcal{T}| \ll 1$ we derive from Eq. (31) with accuracy to leading terms

$$s = (d - 1)\mathcal{T}/2 + c_1\Delta + c_3\Delta^3 - \varrho^2/4T_s + \cdots, \quad (36)$$

whence, substituting here the condition $s_f = 0$, we find the asymptotic law of front evolution

$$-\left(\frac{\Delta_f}{\Delta_f^m}\right)^3 + \left(\frac{\varrho_f}{\varrho_f^m}\right)^2 = (1 + \zeta_f + \cdots)\mathrm{sgn}(\mathcal{T}), \quad (37)$$

where

$$\Delta_f^m = \left[\frac{6(d - 1)T_s^2}{|X_s|}|\mathcal{T}|\right]^{1/3},$$

$$\varrho_f^m = \sqrt{2(d - 1)T_s|\mathcal{T}|},$$

and $\zeta_f = -|X_s|\Delta_f/(d - 1)T_s$ ($|\zeta_f| \ll X_s^2 < 1$). It follows from Eq. (37) that in the domain $\Delta_f < 0, \mathcal{T} > 0$, the two-centered island asymptotically takes the shape of a superellipse (2D) or superellipsoid of revolution (3D), the major semiaxis of which contracts by the law $\Delta_f^m \propto \mathcal{T}^{1/3}$, whereas its minor semiaxis contracts by the law $\varrho_f^m \propto \mathcal{T}^{1/2}$ and, therefore, the aspect ratio of the superellipse (superellipsoid) contracts by the law

$$\mathcal{A} = \varrho_f^m/\Delta_f^m \propto \mathcal{T}^{1/6} \rightarrow 0,$$

as $\mathcal{T} \rightarrow 0$. Thus, we conclude that in 2D and 3D systems, in the domain $\Delta_f < 0$ the island asymptotically takes the shape of a quasi-one-dimensional "string," the length of which contracts unlimitedly by the law $\propto \mathcal{T}^{1/3}$ as $\mathcal{T} \rightarrow 0$. It is remarkable that in the domain $\Delta_f^m \ll \Delta_f \ll T_s|X_s|$ the front remain stationary

$$\varrho_f = \pm\sqrt{|X_s|/3T_s}\Delta_f^{3/2} + \cdots,$$

both before ($\mathcal{T} > 0$) and after ($\mathcal{T} < 0$) the disappearance of the smaller island center, where the front takes the shape of a superhyperbola (2D) or superhyperboloid of revolution (3D), the vertex of which moves toward the larger island center by the law $\Delta_f(\varrho_f = 0) \propto |\mathcal{T}|^{1/3}$ as $|\mathcal{T}|$ increases. It follows from Eqs. (36) and (37) that in the limit of small $\mathcal{T} \rightarrow 0$ the amplitude of the local maximum of $|\varrho_f|$ at $\Delta_{f,\star} = -\sqrt{2T_s\mathcal{T}} + \cdots$ (where $\Delta_{f,\star}$ is the coordinate of the smaller island center) and the amplitude of the local minimum of $|\varrho_f|$ at $\Delta_{f,i} = +\sqrt{2T_s\mathcal{T}} + \cdots$ (where $\Delta_{f,i}$ is the coordinate of the isthmus between the islands) converge to ϱ_f^m by the laws $|\varrho_{f,\star}|/\varrho_f^m = 1 + \mathcal{O}(\mathcal{T}^{1/2})$ and $|\varrho_{f,i}|/\varrho_f^m = 1 - \mathcal{O}(\mathcal{T}^{1/2})$, respectively. In turn, in the limit $\mathcal{T} \rightarrow 0$ the coordinate of island vertex $|\Delta_f|(\varrho_f = 0)$ converges to Δ_f^m much slower, $|\Delta_f|(\varrho_f = 0)/\Delta_f^m = 1 + \mathcal{O}(\mathcal{T}^{1/3})$. Figure 8(a) shows sequential stages of the evolution of 2D island front, calculated from Eq. (20) at $q = 0.5$ and $\Lambda = \Lambda_s$ and demonstrating the key features of island transformation in the vicinity of the critical point T_s, X_s. In the Fig. 8(b), the data of Fig. 8(a) for $\mathcal{T} > 0$ are presented in the scaling coordinates $\varrho_f/\mathcal{T}^{1/2}$ versus $\Delta_f/\mathcal{T}^{1/3}$ that demonstrate the collapse of front profile to the scaling law (37) as $\mathcal{T}, \zeta_f \rightarrow 0$.

3. Self-similar collapse of islands in the range $0 < \chi_c < 1$

It follows from Eqs. (20) and (21) that at $q < 1$, at the collapse points of the larger ($0 < \Lambda < \infty$) and smaller ($0 < \Lambda < \Lambda_s$) islands on the trajectories of the centers $X_\star^+(T)$ and $X_\star^-(T)$, respectively, the parameter χ_c changes within the limits

$$0 < \chi_c(q, \Lambda, d) < 1,$$

whence, according to Eq. (31), at any d at small $\mathcal{T} \ll 1 - \chi_c$ we find

$$s_c = (d - \chi_c)\mathcal{T}/2 + \ldots, \quad c_2 = -(1 - \chi_c)/4T_c + \cdots.$$

At the final collapse stage, in the limit of small

$$\mathcal{T} \ll \frac{T_c(1 - \chi_c)^2}{(d - \chi_c)}\min[\frac{(1 - \chi_c)}{|X_c|^2}, 1],$$
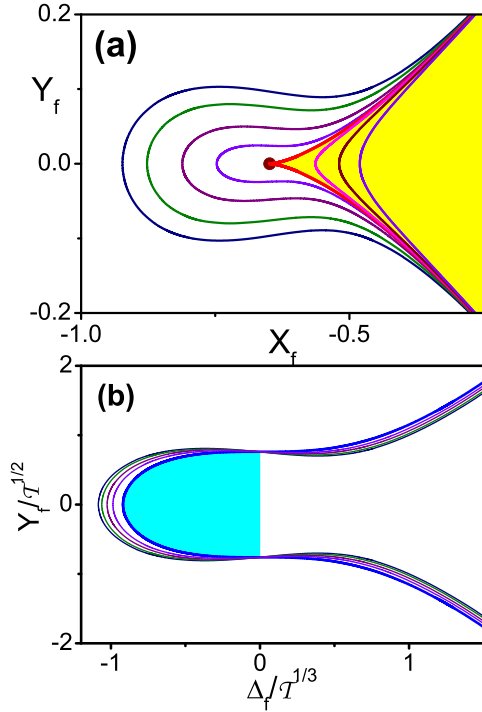
FIG. 8. (a) Evolution of the front of 2D island in the vicinity of the critical point T_s, X_s calculated from Eq. (20) at $q = 0.5$ and $\Lambda = \Lambda_s$: from left to right $\mathcal{T} = 0.01621$, 0.01, 0.004, 0.001, 0, −0.001, −0.004, −0.01. The front at $T = T_s(\mathcal{T} = 0)$ is shown by a thick line. The area of the single-centered island $T > T_s(\mathcal{T} < 0)$ is colored; (b) Data of Fig. 8(a) for $\mathcal{T} > 0$ replotted in the scaling coordinates $\varrho_f/\mathcal{T}^{1/2}$ vs $\Delta_f/\mathcal{T}^{1/3}$: collapse of the front profile to the scaling law (37) as $\mathcal{T} \to 0$. The area of the superellipse $\Delta \leqslant 0$ is colored.

we derive from Eq. (31) with accuracy to leading terms that

$$s = (d - \chi_c)\mathcal{T}/2 + c_2\Delta^2 + \varrho^2/4T_c + \cdots, \quad (38)$$

whence it follows that in 1D systems the fronts $\Delta_f^<$ and $\Delta_f^>$ asymptotically converge symmetrically to the collapse point by the law

$$\Delta_f^{<,>} = \mp\sqrt{2T_c\mathcal{T}} + \cdots.$$

According to Eq. (38), in 2D and 3D systems on the final collapse stage each of the islands takes asymptotically the shape of an ellipse (2D) or ellipsoid of revolution (3D)

$$\left(\frac{\Delta_f}{\Delta_f^m}\right)^2 + \left(\frac{\varrho_f}{\varrho_f^m}\right)^2 = 1 + \cdots \quad (39)$$

the semiaxes of which contract by the laws

$$\Delta_f^m = \sqrt{\frac{2T_c(d - \chi_c)\mathcal{T}}{(1 - \chi_c)}},$$

$$\varrho_f^m = \sqrt{2T_c(d - \chi_c)\mathcal{T}},$$

so that asymptotically each of the islands contracts *self-similarly* up to the collapse point with the time-independent
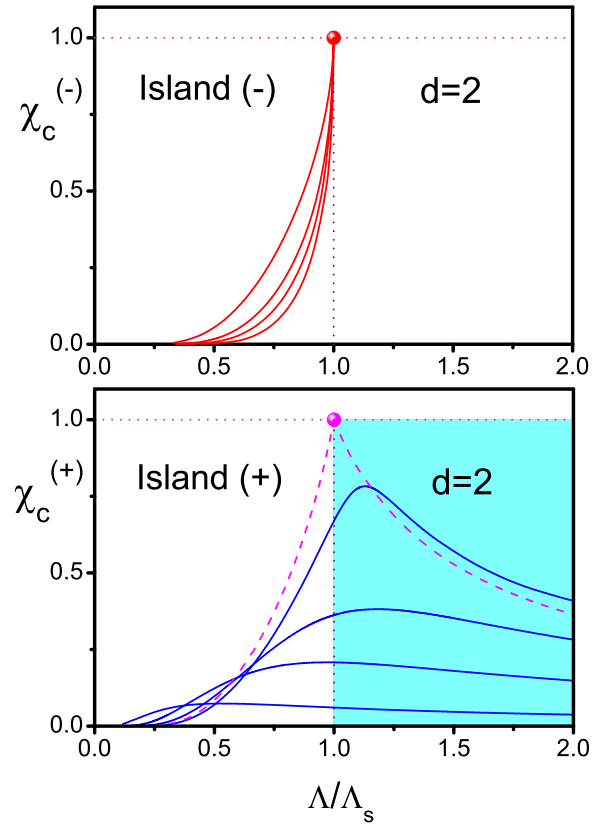

FIG. 9. Dependencies $\chi_c^\pm(\Lambda/\Lambda_s)$ for 2D systems calculated from Eqs. (20) and (21) at $q = 0.9, 0.5, q_\star(2)$ and 0.1 (from top to bottom). The dashed line shows the dependence $\chi_c(\Lambda/\Lambda_s)$ for $q = 1$. Circles mark the critical points $\chi_s = \chi_c(1) = 1$.

aspect ratio

$$\mathcal{A} = \varrho_f^m/\Delta_f^m = \sqrt{1 - \chi_c}.$$

Figures 9 and 10 demonstrate the dependencies $\chi_c^{(\pm)}(\Lambda/\Lambda_s)$ calculated from Eqs. (20) and (21) at several fixed values of q for 2D and 3D systems, respectively. One can see that with an increase in Λ the aspect ratio of the smaller island $\mathcal{A}^{(-)} = \sqrt{1 - \chi_c^{(-)}}$ rapidly decreases from $\mathcal{A}^{(-)}(\Lambda/\Lambda_s \ll 1) \approx 1$ in the domain of autonomous collapse of the islands, where both of the islands contract in the shape of a d-dimensional sphere, to $\mathcal{A}^{(-)}(\Lambda \to \Lambda_s - 0) \to 0$, where the smaller island inherits the shape of a quasi-one-dimensional "string." It is important to note that at the fixed ratio Λ/Λ_s, the aspect ratio $\mathcal{A}^{(-)}$ increases with a decrease in q. The aspect ratio of the larger island $\mathcal{A}^{(+)} = \sqrt{1 - \chi_c^{(+)}}$ demonstrates more nontrivial behavior. It follows from Figs. 9 and 10 that at $q < 1$, with an increase in Λ, the aspect ratio of the larger island passes through the minimum $\text{Min}\mathcal{A}^{(+)} < 1$, which with a decrease in q shifts from the domain of the single-centered island formed by coalescence ($\Lambda > \Lambda_s$) to the domain of individual death of the larger island ($\Lambda < \Lambda_s$) where the "oblateness" of the larger island is formed by depletion of the sea between the islands. As expected, with a decrease in q, the sharp minimum of $\mathcal{A}^{(+)}$ becomes more and more "smooth," and the shape of the island approaches the spherical one: $\text{Min}\mathcal{A}^{(+)} \to 1$ as $q \to 0$.
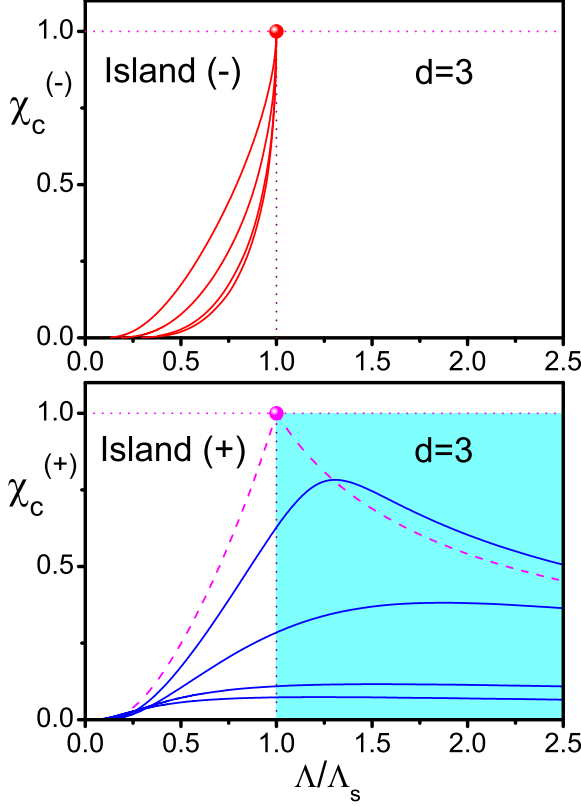
FIG. 10. Dependencies $\chi_c^{\pm}(\Lambda/\Lambda_s)$ for 3D systems calculated from Eqs. (20) and (21) at $q = 0.9, 0.5, q_\star(3)$ and 0.1 (from top to bottom). The dashed line shows the dependence $\chi_c(\Lambda/\Lambda_s)$ for $q = 1$. Circles mark the critical points $\chi_s = \chi_c(1) = 1$.

B. Evolution of islands in the vicinity of coalescence and fragmentation points $\Lambda \geqslant \Lambda_\star$

Let now $\Delta = X - X_{\text{st}}$ and $\mathcal{T} = (T_{\text{st}} - T)/T_{\text{st}}$, where $T_{\text{st}}, X_{\text{st}}|_{\varrho=0}$ are the coordinates of the points of start of coalescence ($T_{\text{st}} = T_{\text{cl}} \leqslant T_M$) or fragmentation ($T_M \leqslant T_{\text{st}} = T_{\text{fr}} < T_s$) of islands on the trajectory of the sea center $s_\star^{(0)}(X_{\text{st}}, T_{\text{st}}) = 0$. It is easy to verify that in the limit of small $\Delta^2/T_{\text{st}} \ll 1$, $\varrho^2/T_{\text{st}} \ll 1$ and $|\mathcal{T}| \ll 1$ we come back again to Eq.(31) where the index "st" arises instead of the index "c."

1. Evolution of 2D and 3D islands at the coalescence threshold $\Lambda = \Lambda_\star$

At the coalescence threshold $\Lambda = \Lambda_\star$, at the point of islands contact we have $X_{\text{st}} = X_M$, $T_{\text{st}} = T_M$, whence, according to Eqs. (26) and (32), it follows

$$\chi_{\text{st}} = \chi_M = d,$$

and for $d > 1$ at small $|\mathcal{T}| \ll 1$ we find

$$s_{\text{st}} = m_M \mathcal{T}^2 + \cdots, \quad c_2 = (d-1)/4T_M + \cdots,$$

where

$$m_M = d[1/T_M - (2d+1)]/4. \tag{40}$$

Thus, in the entire range $0 < q \leqslant 1$ in the limit of small $|\mathcal{T}|$, $|\Delta|$, and $|\varrho|$, we derive from Eq. (31) with accuracy to leading

terms

$$s = m_M \mathcal{T}^2 + c_1 \Delta + c_2 \Delta^2 - \varrho^2/4T_M + \cdots \tag{41}$$

and conclude that at any q, in the vicinity of the island contact point, the distribution of particles in the islands and sea remains invariant with respect to the transformation $\mathcal{T} \rightarrow -\mathcal{T}$, $\Delta \rightarrow -\Delta$. From Eq. (41) it follows that in the vicinity of the contact point the island fronts take the shape of branches of a hyperbola (2D) or hyperboloid of revolution (3D)

$$\frac{(\Delta_f - R\mathcal{T})^2}{\mathcal{D}\mathcal{T}^2} - \frac{\varrho_f^2}{\mathcal{D}(d-1)\mathcal{T}^2} = 1 + \cdots \tag{42}$$

the vertices of which both before ($\mathcal{T} > 0$) and after ($\mathcal{T} < 0$) front contact move along the X axis with a constant velocity by the laws

$$\Delta_f^{\pm} = (R \pm \sqrt{\mathcal{D}})\mathcal{T} + \cdots = (R \pm \sqrt{R^2 - g})\mathcal{T} + \cdots, \tag{43}$$

where

$$R = \frac{d|X_M|}{(d-1)}, \quad g = \frac{4T_M m_M}{(d-1)}. \tag{44}$$

According to Eq. (42), before contact of the fronts $\Delta_f^+ > \Delta_f^-$ ($\mathcal{T} > 0$), whereas after contact of the fronts $\Delta_f^+ < \Delta_f^-$ ($\mathcal{T} < 0$). Therefore, because of the obvious requirement $\Delta_{f,>}^{(-)} \leqslant \Delta_{f,<}^{(+)}$, we conclude that at any q before contact of the fronts ($\mathcal{T} > 0$) the vertices of the smaller and larger islands move by the laws

$$\Delta_{f,>}^{(-)} = (R - \sqrt{\mathcal{D}})\mathcal{T}, \quad \Delta_{f,<}^{(+)} = (R + \sqrt{\mathcal{D}})\mathcal{T},$$

while (due to $\mathcal{T} \rightarrow -\mathcal{T}$, $\Delta \rightarrow -\Delta$ symmetry) after instantaneous contact of the fronts ($\mathcal{T} < 0$), *exchanging their velocities* $V_m^M \leftrightarrow V_p^M$, the vertices of the islands move by the laws

$$\Delta_{f,>}^{(-)} = (R + \sqrt{\mathcal{D}})\mathcal{T}, \quad \Delta_{f,<}^{(+)} = (R - \sqrt{\mathcal{D}})\mathcal{T}.$$

According to Eqs. (40) and (44), with a change in the parameter q from $q = 1$ to $q \rightarrow 0$, the coefficient $m_M(q)$ and, as a consequence, the function $g(q)$ change their sign, $- \rightarrow +$, passing through 0 at the critical value $q_\star$, which, in accordance with Eq. (28), is determined by the requirement $T_M(q_\star) = 1/(2d+1)$. As a consequence, according to Eq. (43), with a change in the parameter q from $q = 1$ to $q \rightarrow 0$, the velocity of the vertex of the smaller island front up to the contact point $V_m^M(q)$ changes its sign, $+ \rightarrow -$, passing through 0 at the critical value $q_\star$: $V_m^M(q_\star) = 0$ ("frozen" vertex). Determining further the ratio of the velocities of vertices of the smaller and larger islands up to the contact point

$$\mathcal{R}(q) = V_m^M(q)/V_p^M(q) = \frac{R - \sqrt{R^2 - g}}{R + \sqrt{R^2 - g}}, \tag{45}$$

we conclude from Eqs. (40), (43), and (44) that with a change in the parameter q from $q = 1$ to $q \rightarrow 0$ this ratio changes monotonically from $\mathcal{R}(1) = -1$ to $\mathcal{R}(q \rightarrow 0) = (d - \sqrt{d})/(d + \sqrt{d}) < 1$ passing through 0 at the critical value $q_\star$. Thus, from Eqs. (42) and (45) we come to the following key conclusions: (1) In the supercritical range $q_\star < q \leqslant 1$, in the vicinity of the contact point, the fronts of the larger and smaller islands move self-similarly to the contact point toward each other with constant velocities, "reflecting" at moment of
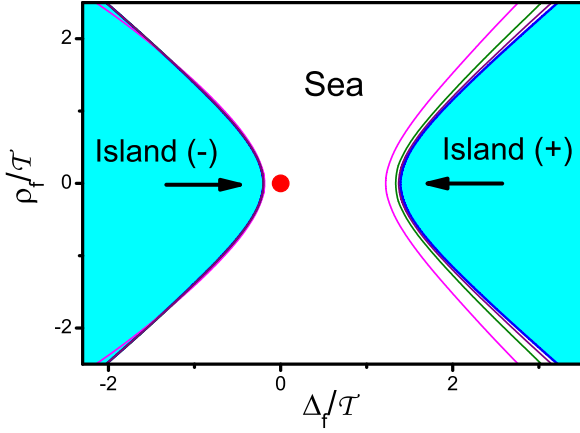
FIG. 11. Evolution of the fronts of 2D islands moving to the contact point in the normalized coordinates $\varrho_f/\mathcal{T}$ vs $\Delta_f/\mathcal{T}$, calculated from Eq. (20) at $q = 0.5$ and $\Lambda = \Lambda_\star$: collapse to the scaling law (42) as $\mathcal{T} \to 0$. Thin lines—$\mathcal{T} = 0.1, 0.03, 0.01$. Thick lines—the scaling law (42). The areas of islands are colored.

contact in the opposite direction with an abrupt "exchange" of velocities. (2) In the subcritical range $0 < q < q_\star$, in the vicinity of the contact point, the fronts of both the larger and smaller islands move self-similarly to the smaller island center with constant velocities both before and after the contact with an abrupt "exchange" of velocities at the moment of islands contact. (3) At any $q < 1$, up to the point of contact, the velocity of the larger island front is always higher in modulus than that of the smaller island front.

Figure 11 presents the evolution of the fronts of 2D islands moving to the contact point in the normalized coordinates $\varrho_f/\mathcal{T}$ versus $\Delta_f/\mathcal{T}$, calculated from Eq. (20) for $q = 0.5$ and $\Lambda = \Lambda_\star$. One can see that the evolution of the "slow" front of the smaller island converges to scaling law (42) much earlier ($\mathcal{T} < 0.1$) than the evolution of the "fast" front of the larger island ($\mathcal{T} < 10^{-2}$). From Eqs. (41) it follows that at the moment $\mathcal{T} = 0$ of contact of the islands in the vicinity $|\Delta_f|, |\varrho_f| \ll T_M$ of the point of contact, the front of each of the islands takes the form of an angle (2D) or cone of revolution (3D) with a vertex at the point of contact and a d-dependent value of the opening angle 2θ, where

$$\tan \theta = |\varrho_f|/|\Delta_f| = \sqrt{(d-1)}. \quad (46)$$

Thus, we conclude that *regardless* of q at the coalescence threshold $\theta_M = \pi/4$ (2D) or $\theta_M = \tan^{-1}\sqrt{2}$ (3D). As an illustration, Fig. 12 shows the shape of 2D islands at the moment of their contact $T = T_M$, calculated from Eq. (20) at $q = 0.5$.

2. Evolution of islands in the vicinity of coalescence and fragmentation points $\Lambda > \Lambda_\star$

From Eqs. (20) and (21) it follows that in the domain $\Lambda > \Lambda_\star$ in the entire range $0 < q \leqslant 1$ on the trajectory of the sea center $X_\star^{(0)}(T)$ at the points of coalescence and fragmentation start $s_\star^{(0)}(X_{st}, T_{st}) = 0$ ($T_{st} = T_{cl} < T_M$, $T_M < T_{st} = T_{fr} < T_s$) the parameter χ_{st} changes within the limits
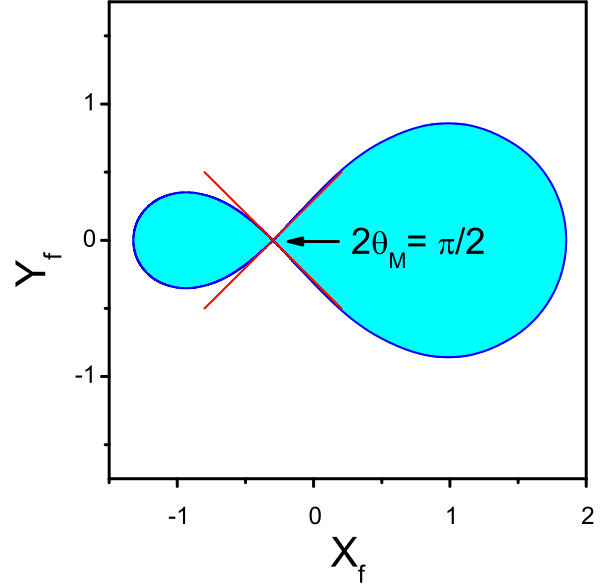
$$d < \chi_{cl} < \infty, \quad 1 < \chi_{fr} < d,$$

FIG. 12. The shape of 2D islands at the moment of their contact $T = T_M$, calculated from Eq. (20) at $q = 0.5$ and $\Lambda = \Lambda_\star$. The areas of islands are colored.

respectively, whence in the limit of small $|\mathcal{T}| \ll |d - \chi_{st}|$, $(\chi_{st} - 1)$ we find

$$s_{st} = \mathcal{T}(d - \chi_{st})/2 + \cdots, \quad c_2 = (\chi_{st} - 1)/4T_{st} + \cdots.$$

Neglecting further shift of the sea center with time $|\Delta| \ll \epsilon|d - \chi_{st}|$ and assuming that

$$|\Delta| \ll \Delta^u = \min[\epsilon(\chi_{st} - 1), \mu\sqrt{\chi_{st} - 1}], \quad (47)$$

where $\epsilon = T_{st}/|X_{st}|\chi_{st}$ and $\mu = 1/\sqrt{|c_4|T_{st}}$, in the limit of small ϱ^2/T_{st} and $|\mathcal{T}|$ we derive from Eq. (31) with accuracy to leading terms

$$s = \mathcal{T}(d - \chi_{st})/2 + c_2\Delta^2 - \varrho^2/4T_{st} + \cdots \quad (48)$$

From Eq. (48) it follows that in 1D systems at any q the fronts of coalescence asymptotically converge symmetrically to the contact point by the laws

$$\Delta_{f,>}^{(-)} = -\sqrt{2T_{cl}\mathcal{T}}, \quad \Delta_{f,<}^{(+)} = +\sqrt{2T_{cl}\mathcal{T}}. \quad (49)$$

Here we focus mainly on the coalescence and fragmentation of 2D and 3D islands that demonstrate a much richer picture of evolution. According to Eq. (48), at $d > 1$ and any q, in the vicinity of contact points the fronts of coalescence and fragmentation take the shape of a hyperbola (2D) or hyperboloid of revolution (3D)

$$\left(\frac{\Delta_f}{\Delta_f^m}\right)^2 - \left(\frac{\varrho_f}{\varrho_f^m}\right)^2 = \mathsf{sgn}[\mathcal{T}(\chi_{st} - d)] + \cdots, \quad (50)$$

where with an increase in T, the semiaxes of the hyperbola (hyperboloid of revolution) first contract ($\mathcal{T} > 0$), and then grow ($\mathcal{T} < 0$) by the laws

$$\Delta_f^m = \sqrt{\frac{2T_{st}|(\chi_{st} - d)\mathcal{T}|}{(\chi_{st} - 1)}}$$
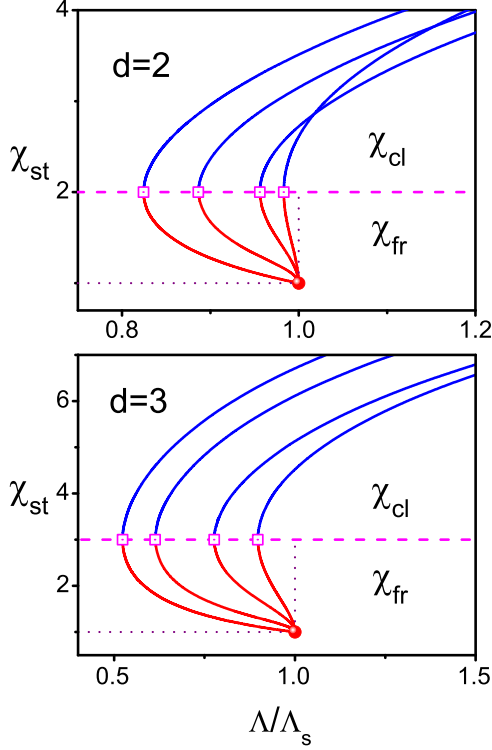
FIG. 13. Dependencies $\chi_{cl}(\Lambda/\Lambda_s)$ and $\chi_{fr}(\Lambda/\Lambda_s)$ calculated from Eqs. (20) and (21) for 2D and 3D systems at $q = 1, 0.9, 0.5,$ and 0.1 (from left to right). Squares and circle mark the critical points $\chi_M = d$ and $\chi_s = 1$, respectively.

and

$$\varrho_f^m = \sqrt{2T_{st}|(\chi_{st} - d)\mathcal{T}|}.$$

According to Eq. (50), in the coalescence domain ($\chi_{cl} > d$) the vertices of the hyperbola (two-sheet hyperboloid) $\pm\Delta_f^m$ move toward each other ($\mathcal{T} > 0$), accelerating, up to the coalescence point $\mathcal{T} = 0$, where the semiaxes Δ_f becomes imaginary and $\varrho_f^m(\mathcal{T} < 0)$ determines a decelerating increase in width (radius) of the isthmus of the formed two-centered island (one-sheet hyperboloid). In the fragmentation domain ($1 < \chi_{fr} < d$), where the two-centered island divides into two separated islands, this process occurs in a reverse order (one-sheet hyperboloid ($\mathcal{T} > 0$) $\to$ two-sheet hyperboloid ($\mathcal{T} < 0$). Figure 13 demonstrates the dependencies $\chi_{cl}(\Lambda/\Lambda_s)$ and $\chi_{fr}(\Lambda/\Lambda_s)$ calculated from Eqs. (20) and (21) for 2D and 3D systems at several values of q. One can see that with an increase in Λ, the quantity χ_{cl} increases unlimitedly from $\chi_M = d$ to ∞ ($\chi_{cl} \propto \ln(\Lambda/\Lambda_s) \to \infty$ as $\Lambda/\Lambda_s \to \infty$), whereas the quantity χ_{fr} decreases from $\chi_M = d$ to $\chi_s = 1$ in the narrower range of Λ, the lower q.

Comparing the reduces velocities of motion of front vertices $|\mathcal{V}_\Delta^m| = |d\Delta_f^m/dT|/\sqrt{|\mathcal{T}|}$ and of increase (contraction) in the radius of the isthmus between the islands $|\mathcal{V}_\varrho^m| = |d\varrho_f^m/dT|/\sqrt{|\mathcal{T}|}$, we find

$$M_m(\chi_{st}) = |\mathcal{V}_\varrho^m|/|\mathcal{V}_\Delta^m| = \sqrt{\chi_{st} - 1}, \tag{51}$$

whence we come to the following conclusions:

(i) In the coalescence domain $d < \chi_{st} = \chi_{cl} < \infty$ at any $0 < q \leqslant 1$ and $d > 1$ the reduced velocity of an increase in the isthmus radius after coalescence start ($\mathcal{T} < 0$) always exceeds the reduced velocity of motion of front vertices to the point of coalescence start ($\mathcal{T} > 0$) increasing unlimitedly with an increase in Λ.

(ii) In the fragmentation domain $1 < \chi_{st} = \chi_{fr} < d$ in 2D systems the reduced velocity of motion of front vertices from the point of fragmentation start ($\mathcal{T} < 0$) always exceeds the reduced velocity of contraction of the isthmus radius to the point of fragmentation start, whereas in 3D systems $M_m > 1$ in the range $2 < \chi_{fr} < 3$ and $M_m \leqslant 1$ in the range $1 < \chi_{fr} \leqslant 2$. The reduced velocity of front motion from the point of fragmentation start increases unlimitedly as Λ approaches the critical value Λ_s.

3. Shape of 2D and 3D islands at the starting points of coalescence T_{fl} and fragmentation T_{fr}

According to Eq. (48), at the moment of islands contact $\mathcal{T}_{st} = 0$, in the vicinity of small $|\Delta|$ satisfying the condition of Eq. (47), the front of each of the islands at any $0 < q \leqslant 1$ takes the form of an angle (2D) or cone of revolution (3D) with a vertex at the point of contact $\Delta = 0$ and the χ_{st} dependent value of opening angle 2θ, where

$$\tan\theta = |\varrho_f|/|\Delta_f| = \sqrt{\chi_{st} - 1}. \tag{52}$$

From Eq. (52) it follows immediately that at any q in the coalescence domain ($T_{cl} < T_M$) the angle $\theta_{cl}(\chi_{cl})$ increases from $\theta_M = \pi/4$ (2D) or $\tan^{-1}\sqrt{2}$ (3D) to $\theta_{cl}(\Lambda \to \infty) = \pi/2$ with an increase in Λ, whereas in the fragmentation domain ($T_M < T_{fr} < T_s$) the angle $\theta_{fr}(\chi_{fr})$ decreases from θ_M to $\theta_{fr}(\Lambda \to \Lambda_s) \to 0$ with an increase in Λ. We conclude thus that, as expected, (a) at any $0 < q \leqslant 1$ and $\Lambda_\star(q) < \Lambda < \Lambda_s(q)$ the angle of coalescence is always grater than that of fragmentation

$$\theta_{cl}(\Lambda, q) > \theta_{fr}(\Lambda, q),$$

and (b) in the limit $\Lambda \to \Lambda_s$ ($\chi_{fr} \to 1$) at the moment of start of fragmentation T_{fr}, in the domain $\Delta \ll \Delta^u$ both of the islands "inherit" the shape of a quasi-1D string $|\varrho_f|/|\Delta_f| \to 0$. As an illustration, Fig. 14 presents the sequential stages of coalescence, fragmentation, and collapse of 2D islands at $\Lambda = 1.62$ and $q = 0.5$, which demonstrate the key features of the evolution of their shape in the range $\Lambda_\star < \Lambda < \Lambda_s$. A remarkable fact should be emphasized that at any $0 < q \leqslant 1$ the angle of the front at the moment of coalescence (fragmentation) start determines unambiguously the ratio of the velocities of growth (contraction) of the isthmus between the islands and motion of front vertices before and after coalescence (fragmentation) start

$$\tan\theta(\chi_{st}) = M_m(\chi_{st}).$$

It remains for us to reveal how the upper boundary of the domain of formation of identical island angles $\Delta^u(q, \Lambda)$ shifts with a decrease in the parameter q, i.e., with an increase in the island asymmetry and corresponding increase in the coalescence threshold $\Lambda_\star$. From Eq. (47) in combination with the requirement $\varrho_f^2/T_{st} \ll 1$, we come to the following conclusions: (1) in the vicinity of the coalescence threshold
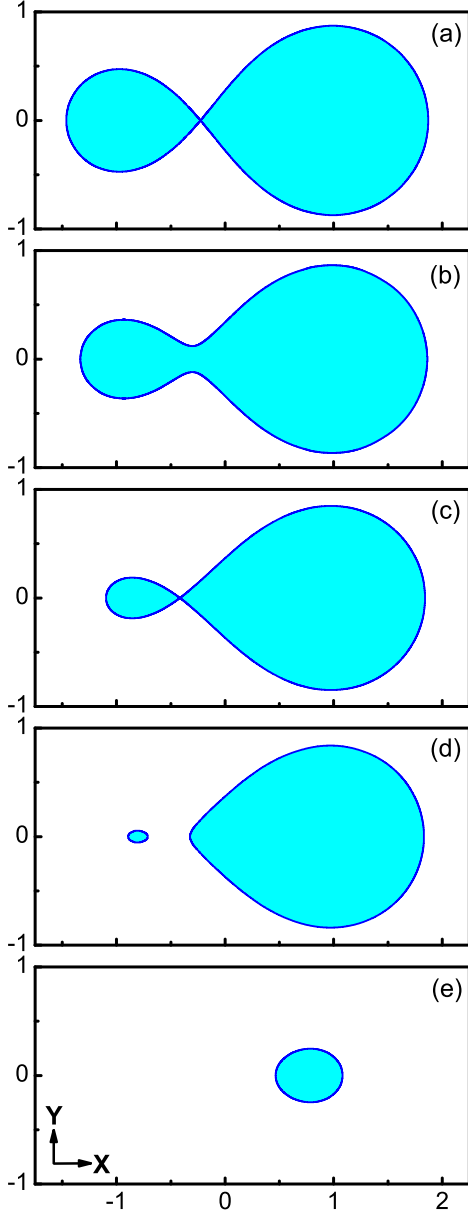
FIG. 14. Sequential stages of coalescence, fragmentation and collapse of 2D islands calculated from Eq. (20) at $\Lambda = 1.62$ and $q = 0.5$ for the time moments $T = T_{\mathrm{cl}} = 0.19650497$ (a), $T = 0.23$ (b), $T = T_{\mathrm{fr}} = 0.26350821$ (c), $T = 0.275$ (d), and $T = 0.55$ (e). The areas of islands are colored.

$|\chi_{\mathrm{st}} - d| \ll 1$, the domain Δ^u logarithmically slowly contracts by the law

$$\Delta^u \propto 1/|\ln q|$$

as $q \to 0$. It is clear that the abnormally slow contraction of the domain Δ^u with an increase in the islands asymmetry is due to a rapid increase in the coalescence threshold $\Lambda_\star \propto 1/q$ that effectively "compensates" for asymmetry increase; (2) in the limit of large $\chi_{\mathrm{cl}} \gg 1$, with an increase in Λ the domain Δ^u logarithmcally slowly contracts by the law

$$\Delta^u \propto 1/\chi_{\mathrm{cl}} \propto 1/\ln(q\Lambda) \propto 1/\ln(\Lambda/\Lambda_s)$$

as $\Lambda/\Lambda_s \to \infty$; (3) in the vicinity of the critical fragmentation point $(\chi_{fr} - 1) \ll 1$, with an increase in Λ the domain Δ^u rapidly contracts by the law

$$\Delta^u \propto (\chi_{fr} - 1)/|\ln q|$$

as $\Lambda/\Lambda_s \to 1$.

V. EVOLUTION AND DELOCALIZATION OF THE REACTION FRONT

One of the key requirements that underlies the results of previous sections is the assumption that the reaction front is sharp enough and, as a consequence, the front moves quasistatically up to a narrow vicinity of the island collapse point. We have demonstrated in Ref. [36] that in the mirror-symmetrical limit $q = 1$ this assumption is realized in a wide range of parameters and, therefore, the whole picture of island evolution is completely self-consistent. In this section, we will be primarily interested in revealing (a) the parameter domain within which the front delocalization occurs at the final (self-similar) collapse stage where the front width grows unlimitedly as T approaches the collapse point T_c and (b) the parameter domain within which front delocalization occurs in a narrow vicinity of the points of coalescence T_{cl} where the front width increase unlimitedly as the front approaches the point of contact.

In Refs. [17,18,21,22] it has been established that at $d > 2$ in the dimensional variables the dependence of the quasistatic front width w on the boundary current density J is described by the mean-field law

$$w_{\mathrm{MF}} \sim (D^2/kJ)^{1/3}. \tag{53}$$

As well as in Ref. [36], to avoid unnecessary complications, we will consider evolution of the front in the mean-field regime for quasi-1D, quasi-2D, and 3D systems. According to Eq. (53), in the units that we have accepted, the mean-field front width takes the form

$$w \sim 1/(\kappa J)^{1/3}, \tag{54}$$

where the effective reaction constant

$$\kappa = kb_0\ell^2/D$$

and the boundary current density

$$J = |\boldsymbol{\nabla} s||_{\mathbf{r_f}} = [\sqrt{(\partial_X s)^2 + (\partial_\varrho s)^2}]|_{\mathbf{r_f}}.$$

A. Self-similar collapse of the smaller island at $\Lambda < \Lambda_s$

From Eqs. (38) and (54) we find that on the final self-similar collapse stage the relative width of the reaction front along the X axis increases by the law

$$\eta_\Delta^m = w_\Delta/\Delta_f^m = \left(\frac{\mathcal{T}_\Delta^Q}{\mathcal{T}}\right)^{2/3}, \tag{55}$$

where the characteristic time of front delocalization is

$$\mathcal{T}_\Delta^Q = \sqrt{\frac{(1 - \chi_c)}{2\kappa T_c(d - \chi_c)^2}}. \tag{56}$$

In the quasi-2D and 3D systems Eqs. (55) and (56) determine the evolution of the relative front width along the major semiaxis of the ellipse (ellipsoid), whereas the evolution of the relative front width along the minor semiaxis of the ellipse (ellipsoid) is determined by the law

$$\eta_\varrho^m = w_\varrho / \varrho_f^m = \left(\frac{\mathcal{T}_\varrho^Q}{\mathcal{T}} \right)^{2/3}, \tag{57}$$

where the characteristic time of front delocalization is

$$\mathcal{T}_\varrho^Q = 1 / \sqrt{2\kappa T_c (d - \chi_c)^2}. \tag{58}$$

According to Eqs. (56) and (58) $\mathcal{T}_\Delta^Q / \mathcal{T}_\varrho^Q = \sqrt{1 - \chi_c} < 1$, whence it follows that the upper limit of front delocalization is determined by the characteristic time of delocalization along the minor semiaxis of the ellipse (ellipsoid). Our goal will be to reveal the domain $\chi(q, \Lambda, d)$ within which, in the diffusion-controlled limit of large $\kappa \gg 1$, the regime of self-similar collapse of the smaller island is reached long before front delocalization.

1. Quasi-1D systems

According to Eq. (38), in quasi-1D systems, the condition of reaching the self-similar collapse of an island in the sharp-front regime in the vicinity of the critical point $1 - \chi_c \ll 1$, where this condition becomes the most "rigid," reduces to the requirement

$$\mathcal{T}_\Delta^Q \ll T_c (1 - \chi_c) \mathsf{min}[(1 - \chi_c) / |X_c|^2, 1],$$

whence, according to Eq. (56), in the limit of small $1 - q \ll 1$ we find

$$1 - \chi_c \gg \kappa^{-1/3}$$

and

$$\mathcal{T}_\Delta^Q \ll \kappa^{-1/3}.$$

In the opposite limit of small $q \ll 1$, we find

$$1 - \chi_c \gg |\ln q|^{3/5} / \kappa^{1/5},$$

whence it follows

$$\mathcal{T}_\Delta^Q \ll |\ln q|^{1/5} / \kappa^{2/5}.$$

2. Quasi-2D and 3D systems

According to Eq. (38), in quasi-2D and 3D systems, the condition of reaching the self-similar collapse of an island in the sharp-front regime in the vicinity of the critical point $1 - \chi_c \ll 1$ reduces to the requirement

$$\mathcal{T}_\varrho^Q \ll T_c (1 - \chi_c)^2 \mathsf{min}[(1 - \chi_c) / |X_c|^2, 1],$$

whence, according Eq. (58), in the limit of small $1 - q \ll 1$ we find

$$1 - \chi_c \gg \kappa^{-1/4}$$

and

$$\mathcal{T}_\varrho^Q \propto \kappa^{-1/2}.$$

In the opposite limit of small $q \ll 1$ we find

$$1 - \chi_c \gg \sqrt{|\ln q|} / \kappa^{1/6},$$

whence it follows,

$$\mathcal{T}_\varrho^Q \propto (|\ln q| / \kappa)^{1/2}.$$

Thus, we conclude that although in the limit of small q the delocalization domain expands, at sufficiently large values of the effective reaction constant $\kappa \gg 1$ the domain of self-similar collapse of an island in the sharp-front regime extends up to a narrow vicinity of the critical point $1 - \chi_c \ll 1$ in a wide range of q.

B. Collapse of the smaller island at the critical point $\Lambda = \Lambda_s$

1. Quasi-1D systems

From Eqs. (33) and (54) we find that on the final collapse stage the relative width of the reaction fronts $\Delta_{f,<}^\pm$ increases by the law

$$\eta_\Delta = w_\Delta / |\Delta_f^\pm| = \left(\frac{\mathcal{T}_\Delta^Q}{\mathcal{T}} \right)^{5/6},$$

where the characteristic time of front delocalization is

$$\mathcal{T}_\Delta^Q \sim 1 / \left(\kappa T_s^{1/2} |X_s| \right)^{2/5}. \tag{59}$$

According to Eq. (33), at the critical point $\Lambda = \Lambda_\star = \Lambda_s$ the condition of reaching the final stage of island collapse in the sharp-front regime reduces to the requirement

$$\mathcal{T}_\Delta^Q \ll T_s |X_s|^2,$$

from which it follows,

$$T_s^{1/2} |X_s| \gg 1 / \kappa^{1/6}, \quad \mathcal{T}_\Delta^Q \ll \kappa^{-1/3}. \tag{60}$$

From Eq. (60), in the limit of small $1 - q \ll 1$ we find

$$1 - q \gg 1 / \sqrt{\kappa},$$

whereas in the opposite limit of small $q \ll 1$ we obtain

$$|\ln q| \ll \kappa^{1/3}.$$

2. Quasi-2D and 3D systems

From Eqs. (36) and (54) we find that at the final self-similar collapse stage, the relative width of the reaction front along the major semiaxis of the superellipse (sulerellipsoid) ($\Delta < 0$) increases be the law

$$\eta_\Delta^m = w_\Delta / \Delta_f^m = \left(\frac{\mathcal{T}_\Delta^Q}{\mathcal{T}} \right)^{5/9},$$

where the characteristic time of front delocalization is

$$\mathcal{T}_\Delta^Q \sim \left(\frac{|X_s|^2}{T_s^4 \kappa^3} \right)^{1/5},$$

whereas the relative width of the reaction front along the minor semiaxis of the superellipse (superellipsoid) ($\Delta = 0$) increases by the law

$$\eta_\varrho = w_\varrho / \varrho_f^m = \left(\frac{\mathcal{T}_\varrho^Q}{\mathcal{T}} \right)^{2/3},$$

where the characteristic time of front delocalization is

$$\mathcal{T}_\varrho^Q \sim (\kappa T_s)^{-1/2}.$$

According to Eq. (36), at the critical point $\Lambda = \Lambda_s$ the condition of reaching the final stage of island collapse in the sharp-front regime reduces to the requirement

$$\max\left(\mathcal{T}_\Delta^Q, \mathcal{T}_\varrho^Q\right) \ll T_s |X_s|^4,$$

whence it follows that the self-similar collapse of the superellipse (superellipsoid) occurs in the sharp-front regime under the condition

$$T_s^{3/4} |X_s|^2 \gg 1/\kappa^{1/4}. \tag{61}$$

From Eq. (61), in the limit of small $1 - q \ll 1$ we find

$$1 - q \gg 1/\kappa^{3/8},$$

whereas in the opposite limit $q \ll 1$ we derive

$$|\ln q| \ll \kappa^{1/3}.$$

Thus, we conclude that in the limit of large κ, at the critical point $\Lambda = \Lambda_s$ the collapse of the superellipse (superellipsoid) in the sharp front regime is reached in a wide range of q.

C. Front delocalization in the vicinity of island coalescence point $\Lambda > \Lambda_\star$

From Eqs. (48), (50), and (54) we find that on the final self-similar stage of opposing motion of the vertices of the fronts $\Delta_f^m(\mathcal{T} > 0)$ to the point of coalescence start, the relative width of the reaction front in the vicinity of the vertices increases by the law

$$\eta_\Delta^m = w_\Delta / \Delta_f^m = \left(\frac{\Delta^Q}{\Delta_f^m}\right)^{4/3} = \left(\frac{\mathcal{T}_\Delta^Q}{\mathcal{T}}\right)^{2/3}, \tag{62}$$

where the characteristic "length" of front delocalization is

$$\Delta^Q \sim \left[\frac{T_{\rm cl}}{\kappa(\chi_{\rm cl} - 1)}\right]^{1/4}, \tag{63}$$

and the characteristic time of front delocalization is

$$\mathcal{T}_\Delta^Q \sim \sqrt{\frac{(\chi_{\rm cl} - 1)}{\kappa T_{\rm cl}(\chi_{\rm cl} - d)^2}}. \tag{64}$$

Thus, according to Eq. (48), we conclude that the self-similar stage of Eq. (50) is reached in the sharp-front regime under the condition

$$\Delta^Q \ll \Delta^u, \epsilon(\chi_{\rm cl} - d).$$

1. Front delocalization in the limit $\Lambda \gg \Lambda_\star$

Far away from the coalescence threshold $\Lambda \gg \Lambda_\star$, $\chi_{\rm cl} \gg \chi_M = d$, it obviously follows that $T_{\rm cl} \ll T_M$, where T_M changes from $T_M \sim 1/2d$ at $1 - q \ll 1$ to $T_M \sim 1/|\ln q|$ at $q \ll 1$. Thus, we conclude that far away from the coalescence threshold $\chi_{\rm cl} \sim 1/T_{\rm cl}$, whence, according to Eqs. (47) and (63), we derive

$$\Delta^Q \sim \left(T_{\rm cl}^2/\kappa\right)^{1/4} \ll T_{\rm cl}$$

and finally find

$$\kappa^{-1/2} \ll T_{\rm cl} \ll T_M, \quad \mathcal{T}_\Delta^Q \sim \kappa^{-1/2}. \tag{65}$$

It follows from Eq. (65) that in the diffusion-controlled limit of large κ the self-similar asymptotics (50) is reached in the sharp-front regime in a wide range of q.

2. Front delocalization in the vicinity of coalescence threshold $\chi_{cl} - d \ll 1$

(a) Quasi-1D systems. In the vicinity of coalescence threshold $\chi_{\rm cl} - 1 \ll 1$, we find from Eqs. (47) and (63) that in the limit of small $1 - q \ll 1$ the asymptotics (50) is reached in the sharp-front regime under the condition

$$\chi_{\rm cl} - 1 \gg \kappa^{-1/3},$$

whence it follows $\mathcal{T}_\Delta^Q \ll \kappa^{-1/3}$. In the opposite limit $q \ll 1$ we find from Eqs. (47) and (63)

$$\chi_{\rm cl} - 1 \gg (|\ln q|^3/\kappa)^{1/5},$$

from which it follows that $\mathcal{T}_\Delta^Q \ll (|\ln q|/\kappa^2)^{1/5}$.

(b) Quasi-2D and 3D systems. In the vicinity of coalescence threshold $\chi_{\rm cl} - d \ll 1$, satisfying the requirements $\mathcal{T}_\Delta^Q \ll \chi_{\rm cl} - d$ and $\Delta^Q \ll \epsilon(\chi_{\rm cl} - d)$, we find that in the limit of small $1 - q \ll 1$ the asymptotics (50) is reached in the sharp-front regime under the condition

$$\chi_{\rm cl} - d \gg \kappa^{-1/4},$$

whence it follows that $\mathcal{T}_\Delta^Q \ll \kappa^{-1/4}$. In the opposite limit $q \ll 1$, we find

$$\chi_{\rm cl} - d \gg (|\ln q|^3/\kappa)^{1/4},$$

from which it follows $\mathcal{T}_\Delta^Q \ll (|\ln q|\kappa)^{-1/4}$. We conclude that in the diffusion-controlled regime of large κ in a wide range of q the asymptotics (50) is reached in the sharp-front regime up to a narrow vicinity of the coalescence threshold $\chi_{\rm cl} - d \ll 1$.

3. Diffusion-controlled annihilation regime

In the diffusion-controlled limit, the mean-field constant of pair annihilation is determined by the expression $k = \zeta D r_a$, where r_a is the annihilation radius and $\zeta = 8\pi$. Thus, for the effective reaction constant in quasi-1D, 2D, and 3D systems, we obtain

$$\kappa = \zeta r_a b_0 \ell^2, \tag{66}$$

whence it follows that at fixed r_a and ℓ, the effective reaction constant is determined unambiguously by the initial sea density. Taking for illustration the realistic values $r_a \sim 10^{-8}$ cm, $b_0 \sim 10^{20}$ cm^{-3}, and $\ell \sim 10$ cm we find $\kappa \sim 10^{15}$, whence it follows that in the diffusion-controlled regime the effective reaction constant is very large in a wide range of b_0 and ℓ. As a consequence, we conclude that in a wide range of b_0, ℓ and q the front remains sharp up to a narrow vicinity of coalescence, fragmentation, and collapse points.

Completing this chapter, we will not dwell here on the details of front relocalization in the processes of growth of the isthmus between the islands and fragmentation (division) of the two-centered island, which have been analyzed in detail in Ref. [36] for mirror-symmetrical islands. It is easy to demonstrate from Eqs. (48) and (50) that at sufficiently large κ these processes occur in the sharp-front regime in a wide range of the parameter q up to a narrow vicinity of coalescence

and fragmentation points and, therefore, the whole picture of island evolution presented above is completely self-consistent.

VI. CONCLUSION

In this work, we have presented a systematic analytical study of diffusion-controlled evolution, coalescence, fragmentation, and collapse of two *nonidentical* spatially separated d-dimensional A-particle islands in the B-particle sea at propagation of the sharp reaction front $A + B \rightarrow 0$. The obtained self-consisted picture of the evolution of the islands and front trajectories is based on the condition of local conservation of the difference concentration $s(\mathbf{r}, t)$ which follows from the "standard" requirement of equality of unlike particles diffusivities and on the assumption that the relative front width can be neglected during islands evolution which follows from the remarkable property of effective dynamical "repulsion" of unlike species. The key features of the rich picture of evolution of the islands and front trajectories can be formulated as follows:

(1) It has been established that if the initial distance between the centers of the islands 2ℓ and the initial ratio of island to sea concentrations are relatively large, depending on the system dimension the evolution of the island-sea-island system is determined unambiguously by two dimensionless parameters $\Lambda = \mathcal{N}_0^+/\mathcal{N}_\Omega$ and $q = \mathcal{N}_0^-/\mathcal{N}_0^+$, where $\mathcal{N}_0^+$ and $\mathcal{N}_0^-$ are the initial particle numbers in the larger and smaller of the islands, respectively, and $\mathcal{N}_\Omega$ is the initial number of sea particles in the volume $\Omega = (2\ell)^d$.

(2) It has been shown that regardless of d, the trajectories of the centers of the islands and sea are determined unambiguously by the parameter q and found that at each fixed $0 < q \leqslant 1$ there are threshold values $\Lambda_\star(q)$ and $\Lambda_s(q) \geqslant \Lambda_\star(q)$ that depend on the dimension and separate the domains of individual death of each of the islands $\Lambda < \Lambda_\star(q)$, coalescence and subsequent fragmentation (division) of the two-centered island $\Lambda_\star(q) < \Lambda < \Lambda_s(q)(d \geqslant 2)$, and collapse of the single-centered island formed by coalescence $\Lambda > \Lambda_s$. It has been demonstrated that with the decreasing parameter q, the thresholds of coalescence $\Lambda_\star(q)$ and of the single-centered island formation $\Lambda_s(q)$ rapidly increase,

changing in the limit of small $q \ll 1$ by the law

$$\Lambda_\star(q), \Lambda_s(q) \propto 1/q |\ln q|^{d/2}.$$

(3) A remarkable fact has been discovered that the evolution of particle concentration in the system center $\mathbf{r} = \mathbf{0}$ is determined unambiguously by only the reduced total initial number of A-particles in the islands $\Sigma = \Lambda(1 + q) = (\mathcal{N}_0^+ + \mathcal{N}_0^-)/\mathcal{N}_\Omega$ *regardless* of how these particles are distributed between the islands. As a consequence, although with a change in q the front trajectories change drastically, above some threshold value $\Sigma_\star(d)$ the times of the direct and inverse passage of the larger island front through the system center become the universal functions of Σ.

(4) A detailed picture of the evolution of the front trajectories with an increase in Λ has been revealed and scaling laws of the evolution of the fronts in the vicinity of collapse, coalescence, and fragmentation points has been found for arbitrary $q < 1$. Among a number of important consequences of the presented analysis, it has been established that the picture of island coalescence qualitatively changes below some critical value $q_\star(d)$.

(5) Within the QSA, the self-consistent power laws of evolution of the relative front width in the vicinity of coalescence and collapse points have been revealed for quasi-1D, quasi-2D and 3D systems. The characteristic times of front delocalization have been obtained depending on the defining parameters of the problem. It has been shown that in the diffusion-controlled annihilation regime, the fronts remains sharp up to a narrow vicinity of coalescence and collapse points and, consequently, the whole picture is self-consistent in a wide range of q.

In conclusion, we hope that the future extensive numerical calculations together with the corresponding experimental data will enable revealing a comprehensive picture of evolution of the front during its delocalization and allow us to reveal the limits of applicability of the macroscopic diffusion description in the vicinity of the collapse point [37].

[1] P. L. Krapivsky, E. Ben-Naim, and S. Redner, *A Kinetic View of Statistical Physics* (Cambridge University Press, Cambridge, UK, 2010).

[2] U. C. Täuber, M. Howard, and B. P. Vollmayr-Lee, J. Phys. A: Math. Gen. **38**, R79 (2005).

[3] D. ben Avraham and S. Havlin, *Diffusion and Reactions in Fractals and Disordered Systems* (Cambridge University Press, Cambridge, UK, 2000).

[4] D. C. Mattis and M. L. Glasser, Rev. Mod. Phys. **70**, 979 (1998).

[5] B. Chopard and M. Droz, *Cellular Automata Modelling of Physical Systems* (Cambridge University Press, Cambridge, UK, 1998).

[6] E. Kotomin and V. Kuzovkov, *Modern Aspects of Diffusion Controlled Reactions: Cooperative Phenomena in Bimolecular Processes* (Elsevier, Amsterdam, 1996).

[7] L. V. Butov, A. C. Gossard, and D. S. Chemla, Nature (London) **418**, 751 (2002).

[8] D. Snoke, S. Denev, Y. Liu, L. Pfeiffer, and K. West, Nature (London) **418**, 754 (2002).

[9] S. Yang, L. V. Butov, L. S. Levitov, B. D. Simons, and A. C. Gossard, Phys. Rev. B **81**, 115320 (2010).

[10] T. Antal, M. Droz, J. Magnin, and Z. Racz, Phys. Rev. Lett. **83**, 2880 (1999).

[11] Z. Racz, Physica A **274**, 50 (1999).

[12] S. Thomas, I. Lagzi, F. Molnar, Jr., and Z. Racz, Phys. Rev. Lett. **110**, 078303 (2013).

[13] F. Brau, G. Schuszter, and A. De Wit, Phys. Rev. Lett. **118**, 134101 (2017).

[14] V. Loodts, P. M. J. Trevelyan, L. Rongy, and A. De Wit, Phys. Rev. E **94**, 043115 (2016).

[15] A. Comolli, A. De Wit, and F. Brau, Phys. Rev. E **100**, 052213 (2019).

[16] I. Mastromatteo, B. Toth, and J. P. Bouchaud, Phys. Rev. Lett. **113**, 268701 (2014).

[17] L. Galfi and Z. Racz, Phys. Rev. A **38**, 3151 (1988).

[18] S. Cornell and M. Droz, Phys. Rev. Lett. **70**, 3824 (1993).

[19] B. P. Lee and J. Cardy, Phys. Rev. E **50**, R3287(R) (1994).

[20] G. T. Barkema, M. J. Howard, and J. L. Cardy, Phys. Rev. E **53**, R2017 (1996).

[21] E. Ben-Naim and S. Redner, J. Phys. A: Math. Gen. **25**, L575 (1992).

[22] Z. Koza, J. Stat. Phys. **85**, 179 (1996).

[23] B. M. Shipilevsky, Phys. Rev. E **67**, 060101(R) (2003).

[24] B. M. Shipilevsky, Phys. Rev. E **70**, 032102 (2004).

[25] B. M. Shipilevsky, Phys. Rev. E **77**, 030101(R) (2008).

[26] S. Kisilevich, M. Sinder, J. Pelleg, and V. Sokolovsky, Phys. Rev. E **77**, 046103 (2008).

[27] B. M. Shipilevsky, Phys. Rev. E **79**, 061114 (2009).

[28] B. M. Shipilevsky, Phys. Rev. E **82**, 011119 (2010).

[29] C. P. Haynes, R. Voituriez, and O. Benichou, J. Phys. A: Math. Theor. **45**, 415001 (2012).

[30] B. M. Shipilevsky, Phys. Rev. E **88**, 012133 (2013).

[31] B. M. Shipilevsky, Phys. Rev. E **95**, 062137 (2017).

[32] M. Fialkowski, A. Bitner, and B. A. Grzybovski, Phys. Rev. Lett. **94**, 018303 (2005).

[33] I. Lagzi, P. Papai, and Z. Racz, Chem. Phys. Lett. **433**, 286 (2007).

[34] N. Withers, Nat. Chem. **2**, 160 (2010).

[35] A. Abi Mansour and M. Al-Ghoul, Phys. Rev. E **89**, 033303 (2014).

[36] B. M. Shipilevsky, Phys. Rev. E **100**, 062121 (2019).

[37] R. Tiani and L. Rongy, Phys. Rev. E **100**, 030201(R) (2019).